CrossMark

ORIGINAL PAPER

Seasonal phenology of appendicularian tunicates in the North Water, northern Baffin Bay

D. Deibel[1] · P. A. Saunders[1,2] · C. J. Stevens[1,3]

Abstract Appendicularian tunicates are marine, gelatinous zooplankton that are important grazers of protists and phytoplankton in Arctic polynyas. However, little is known at the seasonal scale about their life cycle and population phenology in the Arctic. The temporal and spatial pattern of abundance and biomass, body size, and maturity stage were determined over two cruises representing an entire productive season of the North Water (NOW), to determine when and where populations spawn, and whether population growth tracks the expansion of open water and the development of diatom blooms. *Oikopleura vanhoeffeni* began to spawn in April and May, in association with an early diatom bloom caused by the opening of the Jones Sound and Inglefield Bay polynyas in the central NOW. *Fritillaria borealis* began population growth in June, during the transition from the early diatom bloom to an extended bloom of *Chaetoceros socialis* ('C-bloom'). Subsequent spawning and population growth of both species followed the progression of open water and the developing C-bloom, to the north and then south during June–September. Maximum abundance and biomass of both species occurred during September, supported by the C-bloom prey community. Temperature had a strong, positive relationship with the abundance and biomass of both species, and moderate-to-high concentrations of diatoms seemed necessary for the initiation of spawning in *O. vanhoeffeni*. Appendicularians matured quickly in the early-opening polynyas in the NOW despite very low water temperatures and achieved high population growth rates in response to diatoms produced over an extended growing season (April–September).

Keywords Appendicularia · Phenology · Polynya · Population · Spawning · North Water · Arctic

✉ D. Deibel
ddeibel@mun.ca

1   Department of Ocean Sciences, Memorial University of Newfoundland, St. John's, NL A1C 5S7, Canada

2   Department of Biology, Ashland University, Ashland, OH 44805, USA

3   School of Earth and Ocean Sciences, University of Victoria, 3800 Finnerty Road, Victoria, BC V8P 5C2, Canada

Introduction

The polar oceans and their marginal seas are changing (Post et al. 2013). In the northern hemisphere, the Arctic Ocean has experienced early, substantial warming (Ardynya et al. 2011; Rasmussen et al. 2011; Rabe et al. 2012). Arctic pack ice is decreasing in extent and thickness (Howell et al. 2010; Tamura and Oshima 2011). In the foreseeable future, there will be more open water for longer periods of the year than at present, likely resulting in increases in phytoplankton biomass, until nutrients become limiting (Tremblay et al. 2006; Ardynya et al. 2011).

Arctic polynyas are quasi-permanent, mesoscale areas of open water in the midst of ice-covered seas (Ingram et al. 2002; Tremblay et al. 2002b). They allow the penetration of light into the water column and are hotspots of biological production (Klein et al. 2002; Tremblay et al. 2006). They may act as ecological harbingers of a more open Arctic Ocean in the future (Ingram et al. 2002; Tremblay et al. 2006). Increasing extent and duration of open water may affect the abundance and species diversity of Arctic

Ocean consumers and, in turn, trophic relationships. Thus, it is important to understand how present-day polynya food webs function (Pesant et al. 1998, 2000; Berreville et al. 2008).

The North Water (NOW) is the name given to the northern extremity of Baffin Bay, between Ellesmere and Devon islands, Canada, and north-western Greenland. In late winter and spring, the NOW typically contains three large polynyas in and immediately outside the mouths of Smith Sound, Inglefield Bay, and Jones Sound (Richard et al. 1998a; Tang et al. 2004). In June and July, these polynyas generally merge into a large area of open water (Richard et al. 1998a). The NOW is one of the most biologically productive Arctic seas, due to the relatively large area covered by polynyas and to a long productive season, including an extended diatom bloom (Klein et al. 2002; Vidussi et al. 2004; Tremblay et al. 2006). Although phytoplankton production in the NOW supports a complex food web which includes humans (Stirling 1997; Tremblay et al. 2002b), the zooplankton ecology of the NOW has not received the attention given to its physics, chemistry, and phytoplankton ecology. While copepod abundance and feeding have been described for most of the productive season (Ringuette et al. 2002; Saunders et al. 2003; Stevens et al. 2004), appendicularian tunicate abundance and feeding have been described only for *Oikopleura* in July 1998 and September 1999 (Acuña et al. 2002; Deibel et al. 2005). There has not been an investigation of the seasonal phenology of the abundance and biomass of appendicularians, here also including *Fritillaria*, nor of their life history and population dynamics in relation to the changing physical, chemical, and biological environment of the NOW. The present paper addresses these knowledge gaps.

Appendicularian tunicates are ecologically important suspension feeders in all oceans (Fenaux et al. 1998). They use fine mucous filters to collect and ingest a wide size range of particles, from colloids to diatoms (Deibel 1998; Tönnesson et al. 2005). In temperate and boreal waters, the population clearance rates of appendicularians may at times be greater than that of all copepod species combined (Knoechel and Steel-Flynn 1989; Deibel 1998). In addition, given favourable temperature and food concentration, secondary production of appendicularians can be greater than that of herbivorous copepods (Hopcroft and Roff 1995; Nakamura 1998; Choe and Deibel 2011).

Appendicularians can be abundant in Arctic polynyas, forming major links between phytoplankton, protists, and subsequent trophic levels in both the Northeast Water (NEW) (Pesant et al. 1998, 2000; Acuña et al. 1999) and the NOW (Acuña et al. 2002; Booth et al. 2002). Shed appendicularian houses and faeces dominate the vertical flux of biogenic particulate organic matter in the NEW polynya for large portions of the year (Bauerfeind et al.

1997). The appendicularian species reported from polynyas include *Oikopleura vanhoeffeni, Oikopleura labradoriensis,* and *Fritillaria borealis*. In polar oceans, the abundance and biomass of these species are often significantly correlated with environmental conditions, such as temperature, salinity, and food concentration (Blachowiak-Samolyk et al. 2008; Dvoretsky and Dvoretsky 2009). *Oikopleura vanhoeffeni* can be abundant in ice edge habitats, while *F. borealis* seems to thrive primarily in warmer (i.e. >0 °C), ice-free waters (Arashkevich et al. 2002; Hopcroft et al. 2010). However, the seasonal time course of species-specific abundance and biomass of appendicularians has not been examined in a polynya in relation to physical and biological environmental factors.

The coarse-scale pattern of oikopleurid abundance and biomass in the NOW in July and September has been described from a preliminary analysis of upper mixed layer samples by Deibel et al. (2005). The present paper extends this earlier analysis to the full set of samples from the upper 100 m, covering an entire productive season (April–September), and now includes data on *F. borealis*. Multivariate statistical techniques are used to test several hypotheses concerning the seasonal phenology of appendicularian populations. Specifically, (1) when and where do appendicularians spawn in the NOW? (2) Do the abundance and biomass of appendicularians track the spatial and temporal progression of the diatom blooms across the NOW, or are they most abundant in post-bloom waters in which the microbial loop is most important? This hypothesis examines the emerging paradigm that appendicularians are associated with diatom-based, as well as microbial-based, food webs (Lobón et al. 2013). (3) Is there evidence that appendicularians are multivoltine, as are some copepod species in the NOW (Ringuette et al. 2002)? Testing these hypotheses makes use of new information from the samples, not available to Deibel et al. (2005), on the length and maturity stage distributions of oikopleurids. (4) Is *F. borealis* confined to Atlantic source waters (Blachowiak-Samolyk et al. 2008; Dvorestsky and Dvorestsky 2013), or abundant in the NOW generally? Accordingly, is *F. borealis* temporally or spatially segregated from *O. vanhoeffeni* in the NOW, as is the case in Conception Bay, Newfoundland (Choe and Deibel 2008)? This hypothesis tests the applicability of environmental niche theory to sympatric appendicularian species.

Methods

This research was a component of the International North Water Polynya Project (Deming et al. 2002). The general goal of the zooplankton sub-project, of which this study was one part, was to understand the effect of polynya

formation and physical dynamics on the gradients of phytoplankton and protist abundance and size, and the resultant effect of these prey gradients on the abundance, size structure, reproduction, and grazing potential of suspension-feeding copepods and appendicularians.

Sample collection and analytical methods

Data summarized by month represent the following time periods: 4 April 1998–4 May 1998 ('April'), 7 May 1998–31 May 1998 ('May'), 4 June 1998–27 June 1998 ('June'), 1 July 1998–21 July 1998 ('July'), and 27 August 1999–1 October 1999 ('September'). Because relatively few samples were collected in April and May, data collected during these months are combined in some of the tables and figures and are designated 'April–May'. Stations sampled each month varied, depending upon changing ice conditions and scientific objectives.

Collection and analysis of physical, chemical, and phytoplankton samples have been described elsewhere (Klein et al. 2002; Tremblay et al. 2002a, b; Booth et al. 2002). Zooplankton samples were collected by depth-stratified, vertical tows of closing, 6-m-long, Nitex mesh plankton nets (200-µm, 1-m^2 square mouth) (Ringuette et al. 2002), or, from 11 to 30 May 1998, by closing, 300-µm, 0.79-m^2, 1-m-diameter ring nets. The substitution of the 300-µm-mesh net was necessitated by loss of the 200-µm net. The trunk length of newly hatched *O. vanhoeffeni* and *F. borealis* is >200 µm, and with tail and house, ca. 1 mm (Choe and Deibel 2008, 2011). Thus, this change in mesh size was not expected to affect the results. This expectation was confirmed by the abundance time course data (see "Results"). Net tows represented surface, middle, or deep strata, based upon the vertical profiles of temperature, salinity, and fluorescence at each station (Online Resource 1). On-board processing of zooplankton samples has been described elsewhere (Saunders et al. 2003; Deibel et al. 2005).

A Motoda box splitter or Hensen–Stempel pipette was used to remove subsamples from the zooplankton samples. Appendicularians were classified as *F. borealis* or *O. vanhoeffeni*. The congeners *O. vanhoeffeni* and *O. labradoriensis* cannot be easily differentiated in fixed samples. However, based upon distinct temperature–salinity envelopes of these species in cold, Newfoundland coastal waters (Choe and Deibel 2008), the area north of 77°N was most likely unsuitable for *O. labradoriensis* during the study period.

Trunk length of *O. vanhoeffeni* was determined to the nearest 0.1 mm using a Wild stereomicroscope and ocular micrometer. Trunk length was defined as the distance from the tip of the mouth to the posterior edge of the stomach, excluding the gonad. In our net samples, the trunks of

animals were frequently separated from their tails. While trunks are fragile and generally damaged when detached from tails, the tails are muscular and relatively undamaged. The maximum width of detached tails was used to estimate trunk lengths of these specimens from regressions of trunk length versus tail width constructed from intact specimens (Online Resource 2). Observed trunk length was multiplied by a factor of 1.18 to correct for shrinkage of the animals in formalin (Deibel 1988). In addition, maturity stage of *O. vanhoeffeni* was classified following the 5 categories of Shiga (1976) for the congener *O. labradoriensis*, where stage I is newly hatched juveniles, and stage V mature, pre-spawning adults.

In situ appendicularian abundance (m^{-3}) was calculated using tow volume estimates determined from net dimensions, flow meter revolutions, and tow depths, assuming 100% filtration efficiency. Areal abundance and biomass values are reported for all stations and sample dates in which depth-stratified net tows, singly or in combination, covered depths down to at least 100 m. Thus, the abundance and biomass values presented here are not directly comparable to a preliminary analysis of a subset of stations by Deibel et al. (2005), in which only surface tows covering the upper mixed layer were considered. Data are also included for Station 44 in July, where the surface net tow extended to 87 m. In this paper, appendicularian abundances <500 m^{-2} will be referred to as 'low', 500–5000 m^{-2} as 'moderate', and >5000 m^{-2} as 'high'.

Volumetric and areal biomass of *O. vanhoeffeni* (µg C m^{-3} and mg C m^{-2}) were estimated from the trunk length of each animal in a sample using the regression equation of Deibel (1988). Volumetric and areal biomass of *F. borealis* were estimated using the equation of Capitanio et al. (2008), assuming a mean trunk length of 0.7 mm in all samples and carbon = 0.45 × dry weight. Thus, the mean carbon mass fritillarid^{-1} was estimated to be 0.1 µg C in all samples. Because of these assumptions and the use of a constant conversion factor, the spatial pattern of the abundance and biomass of *F. borealis* was identical. In this paper, *O. vanhoeffeni* biomass from 0 to 5 mg C m^{-2} will be referred to as 'low', 5–50 mg C m^{-2} as 'moderate', and >50 mg C m^{-2} as 'high'. Low, moderate, and high biomass categories for *F. borealis* are an order of magnitude lower than those of *O. vanhoeffeni*.

The status of a subset of populations was classified as pre-spawning, spawning, or post-spawning, based upon available maturity stage and trunk length frequency data. Pre-spawning populations were essentially unimodal, predominately maturity stage IV and V. Spawning populations had bimodal maturity stage distributions, with maturity stage I forming the younger mode and stages IV and V comprising the older mode. Trunk length of spawning populations was distributed evenly across most size

categories. Trunk length data alone cannot be used to define a spawning population, because individuals can grow to a large size without maturation (Troedsson et al. 2002; Lombard et al. 2009). Post-spawning populations had essentially unimodal trunk length and maturity stage distributions, dominated by small animals with trunk lengths from 0.3 to 1.0 mm and maturity stages I and II.

Statistical analyses

Spearman's rank–order correlation analyses and PCA bubble plots were used to investigate the relationship between appendicularian abundance, biomass, trunk length, and maturity stage, and the time–space multivariate environmental pattern of stations, as captured in the first 5 PCA axes. All statistical analyses were conducted using Primer-E (version 6.1.16).

First, pairwise relationships between all covariables were examined by making bivariate scatter plots. Most relationships were nonlinear and monotonic. Therefore, the strength of the monotonic relationship among covariables was determined using the nonparametric Spearman's rho statistic. Spearman's rho uses the ranks of the raw data and is insensitive to outliers, which were not removed prior to analysis. Since zeroes in the biological data matrices were ecologically relevant, they were not removed prior to analysis. Empty cells ($n = 6$) in the environmental data matrix were filled by an estimate based upon the nearest samples available in space–time.

Next, all variables were examined for normality and transformed if necessary. Bivariate plots of all variables were then examined pairwise to confirm normality, linearity, and monotonicity. Since environmental variables had various units and may have meaningful zero and negative values, they were normalized before principal component analysis by subtracting each value from the mean and dividing by the standard deviation.

Complete linkage cluster analysis was run on the resemblance matrix of pairwise, Euclidean distances among all stations. Significance level of clusters was determined by SIMPROF, with a priori factors date, day of the year, station, month, and ice cover. Significance of these factors to account for the multivariate environmental pattern was tested by ANOSIM. A multivariate analogue of stepwise multiple regression (BVSTEP, under the BEST routine) was used to select a subset of environmental variables ($n = 6$), which together accounted for 95% of the multidimensional pattern in the PCA. These six variables were: silicate concentration integrated over the upper mixed layer (siluml) and the upper 100 m (sil100), the mean salinity integrated over the euphotic zone (saleuph), the mean temperature integrated over the upper 100 m

(temp100), potential density at the surface (sigthetasurf), and euphotic zone depth (eudepth) (Table 1). All subsequent multivariate analyses and plots were based upon these 'best six' environmental variables.

Study area and oceanographic setting

The North Water (NOW) is located at the northern terminus of Baffin Bay (BB), between Ellesmere and Devon islands, Canada, and north-west Greenland (Fig. 1). The Smith Sound, Jones Sound, and Inglefield Bay polynyas merge into a single polynya in early summer, forming the largest recurrent polynya in the Arctic (80,000 km^2) (Online Resource 3) (Mei et al. 2002; Tremblay et al. 2002b). The Smith Sound polynya is established and maintained by persistent northerly winds, a polar current flowing towards the south, and an ice dam blocking the northern end of Smith Sound (Melling et al. 2001; Marsden et al. 2004; Rasmussen et al. 2011).

Circulation within the NOW is driven by a polar current (PC) flowing southwards through Nares Strait and Smith Sound, and a northern extension of the West Greenland Current (WGC) flowing north-westwards along the Greenland coast (Melling et al. 2001; Aksenov et al. 2010; Rasmussen et al. 2011). Surface-layer current velocities in the PC generally range between 10 and 15 cm s^{-1}, while velocities in the WGC are <5 cm s^{-1} (Melling et al. 2001; Aksenov et al. 2010).

Due to seasonally increasing surface temperature and decreasing salinity, it is problematic to use temperature and salinity to define water masses in sub-Arctic seas (Tremblay et al. 2002a; Bâcle et al. 2002). Tremblay et al. (2002a) developed a nutrient-based index (Si$_{ex}$) which depends upon the silicate and nitrate + nitrite content of water samples to assign them to either polar current, surface water (i.e. silicate-rich Arctic water {SRAW}), or North Atlantic water from the West Greenland Current (i.e. Baffin Bay Water {BBW}). The index, which ranges from 0 (no SRAW) to 1.0 (100% SRAW), is calculated by

$$Si_{ex} = (Si-N) - 1.06/12.75 - 1.06, \quad (1)$$

where Si = the vertically averaged silicate concentration, and N = the vertically averaged nitrate + nitrite concentration over the upper 100 m of the water column. Following Tremblay et al. (2002a), categorical labels of SRAW were assigned to samples with a value of Si$_{ex}$ ≥ 0.70 and BBW to samples with a value of Si$_{ex}$ ≤ 0.30. As many stations contained complex mixtures of SRAW and BBW, the labels SRAW/BBW (i.e. mixed water with SRAW dominant) were assigned to samples with Si$_{ex}$ < 0.70 but ≥0.50 and BBW/SRAW (i.e. mixed water with BBW dominant) to samples with Si$_{ex}$ > 0.30 but <0.50.

Table 1 The best six environmental variables used for the environmental principle components analysis

Variable	Group 1 ('pre-bloom') ($n = 17$)	Group 2 ('T-bloom') ($n = 6$)	Group 3 ('C-bloom') ($n = 30$)	Loading on PC1	Loading on PC2
$Silicate_{100}$	907–2352	544–961	533–2369	0.34	0.59
	1751	666	1168		
	$1686^a \pm 462$	$733^b \pm 173$	$1191^c \pm 445$		
$Salinity_{euph}$	32.60–33.53	32.75–33.46	28.99–32.83	0.39	−0.59
	33.04	33.04	32.11		
	$33.04^a \pm 0.27$	$33.05^a \pm 0.28$	$31.75^b \pm 1.07$		
$Silicate_{uml}$	38.7–1634	6.25–102	4.66–245	0.49	0.25
	686	64.1	20.6		
	$643^a \pm 449$	$57.1^b \pm 38.2$	$49.6^b \pm 66.2$		
$Temp_{100}$	−1.79 to −1.29	−1.42 to −0.13	−1.41 to −0.01	−0.49	−0.14
	−1.63	−1.10	−0.86		
	$-1.61^a \pm 0.16$	$-0.97^b \pm 0.49$	$-0.79^b \pm 0.41$		
$Sigma\text{-}t_{surf}$	25.98–26.96	25.69–26.81	23.59–26.17	0.44	−0.45
	26.50	26.47	25.25		
	$26.48^a \pm 0.27$	$26.39^a \pm 0.41$	$25.27^b \pm 0.73$		
Eudepth	24.6–54.4	17.2–28.6	12.0–45.9	0.25	0.13
	48.5	21.4	32.7		
	$45.5^a \pm 9.67$	$21.9^b \pm 3.72$	$30.7^c \pm 8.25$		

'Group n' is the range (line 1), median (line 2), and mean $\pm$ standard deviation (line 3) of each variable in each of the 3 station groups as defined by cluster analysis and analysis of similarities. 'Loading on PCn' is the loading factor (i.e. the linear coefficient) of each variable on the first two axes of the principle component analysis shown in Fig. 2. Mean values sharing the same lower-case letter were not significantly different ($p > 0.05$, one-way ANOVA and Tukey's LSD test)

$Silicate_{100}$ = the silicate concentration integrated over the upper 100 m (mmol m^{-2}); $Salinity_{euph}$ = the mean salinity of the euphotic zone (i.e. 1% of incident irradiation) (no units); $Silicate_{uml}$ = the silicate concentration integrated over the upper mixed layer (mmol m^{-2}); $Temp_{100}$ = the mean temperature of the upper 100 m (°C); $Sigma\text{-}t_{surf}$ = sea water density at 5 m depth (kg m^{-3}); and Eudepth = depth of the euphotic zone (i.e. 1% of incident irradiation) (m)

The oceanographic phenology during the NOW expedition has been described in several journal publications (see below). The following review is a summary of environmental conditions relevant to appendicularian population dynamics.

The ice dam north of Smith Sound formed in early March 1998 (Wilson et al. 2001; Ingram et al. 2002). This ice dam allowed the Smith Sound polynya (SSP) to be well developed by mid-April, extending further to the south along the Canadian than the Greenland shore. BBW was predominant in the NOW, with SRAW confined to northwestern stations (Tremblay et al. 2002a). The diatom bloom began in late April at eastern stations dominated by BBW (Klein et al. 2002; Vidussi et al. 2004) and on the western side near the Jones Sound polynya (Ringuette et al. 2002; Odate et al. 2002; Booth et al. 2002). Phytoplankton at these stations was dominated by large, centric diatoms and *Thalassiosira* spp. (Lovejoy et al. 2002). Nitrate concentrations were relatively high and non-limiting at all stations, indicating that the phytoplankton bloom was in an early stage.

By early May, the SSP and Inglefield Bay polynyas (IBP) were joined along the Greenland coast, and the Jones Sound polynya (JSP) was well developed south of Coburg Island. All three polynyas merged by late May, with open water again extending much further to the south along the Canadian shore. All the stations in Fig. 1 were in open water by late May, except southern stations. There was an increase in polar outflow in May and June 1998, with SRAW dominating most of the stations in the western half of the NOW (Tremblay et al. 2002a). The phytoplankton bloom accelerated in early May and June along much of the Greenland coast (Vidussi et al. 2004) and central NOW, including station 44 near the mouth of Jones Sound (Tremblay et al. 2002b). Nitrate was depleted in the upper 35 m of the water column in early May at several stations and was low at all stations along the coast of Greenland in June. Concentrations of chlorophyll *a* were maximal in May at eastern stations in BBW and in central NOW stations in June (Klein et al. 2002). From the onset to the peak of the early bloom (May–June), phytoplankton biomass in the eastern NOW (BBW) was dominated by tabular chains
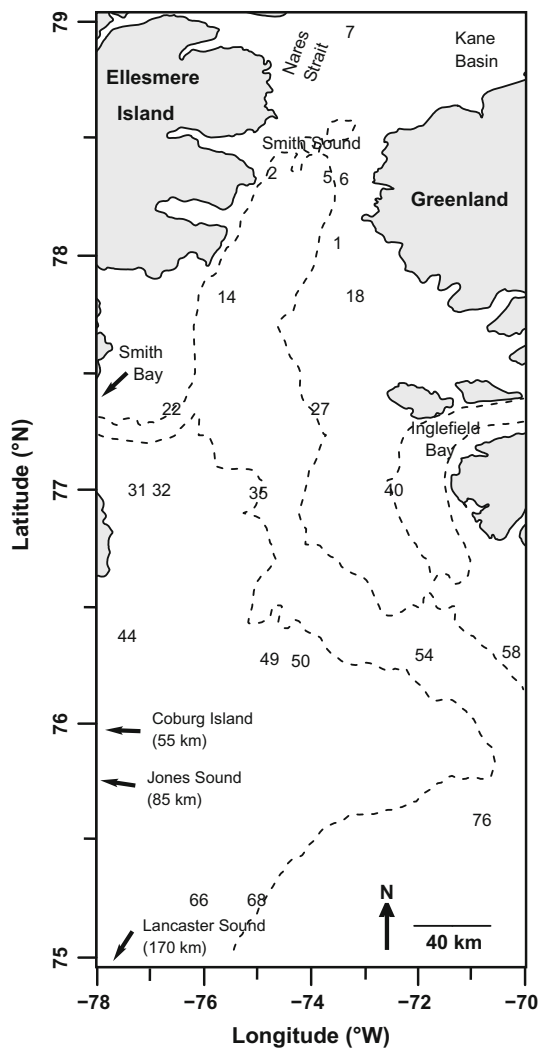
Fig. 1 Stations at which appendicularian samples were collected in the North Water. The 500-m bathymetric contour is shown by a *dotted line*. Spatial nomenclature will follow the convention of 'northern' for latitudes >77.5°N (stations 1–18), 'central' for latitudes from 76 to 77.5°N (stations 22–58), and 'southern' for latitudes <76°N (stations 66–76). Those stations west of −74°W will be referred to as 'western' and stations east of −74°W as 'eastern'

of *Thalassiosira* spp., whereas in the central NOW, there was a more diverse mix of *Thalassiosira* spp., ribbon-forming pennate diatoms, and *Chaetoceros* spp. (Booth et al. 2002; Lovejoy et al. 2002).

The ice dam in Smith Sound broke up in June, with some increase in broken ice along the Greenland coast during July. After break-up of the ice dam, in July 1998, the NOW returned to a state similar to April, with more ice and a greater contribution of BBW to most stations (Tremblay et al. 2002a). Nitrate uptake rates were low at all stations, except for the most northerly stations near Smith Sound. The second, more extended diatom bloom (June–September) was dominated by the small centric diatom *Chaetoceros socialis* and, in one part of the NOW,

by large ciliates and dinoflagellates (Lovejoy et al. 2002; Booth et al. 2002; Tremblay et al. 2002b). In late June and July, the phytoplankton community in the east-central NOW shifted from dominance by diatoms to dominance by flagellates, dinoflagellates, and ciliates (Lovejoy et al. 2002, Vidussi et al. 2004).

In September 1999, the NOW was entirely ice-free south to Lancaster Sound and was dominated by BBW water. Concentrations of chlorophyll *a* were low throughout the NOW, with highest concentrations at northern stations in Smith Sound, where the small centric diatom *C. socialis* remained a dominant member of the phytoplankton community (Booth et al. 2002). The combination of large size, early opening, and the extended bloom of *C. socialis* all contributed to the high biological productivity of the NOW.

Results

Hypotheses concerning environmental pattern

Group-averaged, cluster analysis of environmental data revealed three significantly different groups of stations ($p < 0.001$) (dendrogram not shown). Because of the correspondence between these groups and the floristic observations of Booth et al. (2002), these groups will be referred to as pre-bloom, T-bloom (i.e. the early, transient *Thalassiosira* bloom), and C-bloom (i.e. the later, extended *Chaetoceros* bloom). The T-bloom stations had fourfold to fivefold, and threefold to fourfold, greater mean chlorophyll *a* concentration than the pre-bloom, and C-bloom stations, respectively (Online Resource 4). In addition, T-bloom stations had significantly lower silicate concentrations (sil_{100}) than did the other two groups, and a shallower euphotic zone (Table 1).

Principal component analysis (PCA) resulted in separation of the stations into the pre-bloom group on the right, the T-bloom group in the lower centre, and the C-bloom group on the left (Fig. 2a). Silicate$_{uml}$ concentration and temperature were most strongly loaded on PC1 (Table 1), with temperature decreasing and silicate increasing towards the right. Temperature was nearly colinear with PC1. Silicate concentration$_{100}$ and salinity were most strongly loaded on PC2, with silicate increasing and salinity decreasing upwards (Table 1). Eigenvector plots (not shown) indicated silicate increasing to the upper right of Fig. 2a and decreasing to the lower left, while salinity and density increased to the lower right and decreased to the upper left. Thus, pre-bloom stations were cold with high nutrient concentrations, while C-bloom stations were warmer, fresher and had lower inorganic nutrient concentrations (Table 1). Although there were exceptions, the pre-bloom group contained stations sampled primarily in April

Fig. 2 North Water station groups. Principal component analysis (PCA) based upon Euclidean distances among stations derived from the best six environmental variables. Groups at a distance of 3.1 are shown, based upon a group-averaged cluster analysis (*not shown*). PC1 accounts for ca. 54% of the among-station pattern in the environment, and PC2 ca. 21%. The temporal pattern among stations is shown in panel (**a**), shaded by month. The spatial pattern among stations is shown in panel (**b**), shaded by the water mass proxy variable Si_{ex}. Si_{ex} $1 \geq 70\%$ Baffin Bay water (BBW); Si_{ex} $2 = $ mixed BBW and silicate-rich Arctic water (SRAW), with 50–69% BBW; Si_{ex} $3 = $ mixed BBW and SRAW, with 51–70% SRAW); Si_{ex} $4 \geq 70\%$ SRAW. Pre-bloom = group containing primarily those stations with pre-bloom concentrations of chlorophyll *a* and inorganic nutrients. T-bloom = group containing those stations which were generally characteristic of the early diatom bloom dominated by *Thalassiosira* spp. C-bloom = group containing those stations which were generally characteristic of the extended diatom bloom dominated by *Chaetoceros socialis*. Data plotted are the station numbers referred to in the text
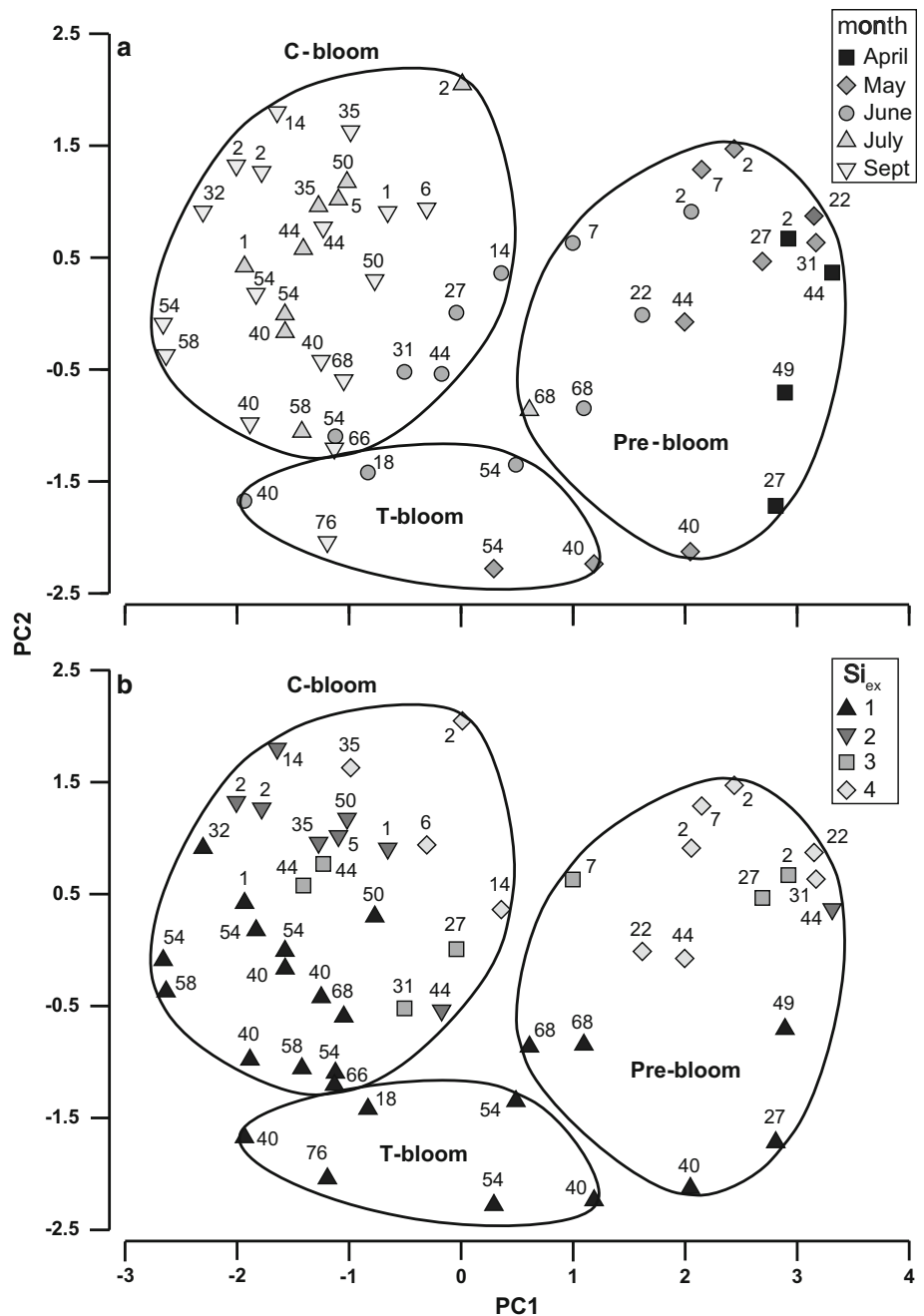
and May ($n = 12$) and the C-bloom group primarily in July and September ($n = 25$) (Fig. 2a). The T-bloom group contained stations sampled in May ($n = 2$), June ($n = 3$), and September ($n = 1$). June was a transitional time, with stations nearly equally divided among pre-bloom ($n = 4$), T-bloom ($n = 3$), and C-bloom ($n = 5$) groups.

The spatial pattern in water masses can be seen by replacing the month code in Fig. 2a with a shading code for the Si_{ex} factor, which accounted for the latitude and longitude patterns in environmental variables (Fig. 2b). Si_{ex} increased from lower left to upper right, indicating the

predominance of BBW stations in the lower left, SRAW stations in the upper right, and the occurrence of the T-bloom primarily in BBW. Thus, PC1 generally reflects the temporal pattern, and PC2 the spatial pattern, of environmental variability. Comparison of Fig. 2a, b indicates that temporal evolution of the environment occurred essentially synchronously over the entire study area (i.e. month symbols were arrayed vertically, except for June, which was a period of rapid environmental transition) (Fig. 2a), while over the entire time of the study, the spatial water mass structure was relatively stable (i.e. the Si_{ex}

symbols were arrayed essentially horizontally) (Fig. 2b). Overall, PCA showed that time (i.e. season) accounted for more of the pattern in the environment (i.e. PC1 accounted for 54% of among-station variability) than did space (i.e. latitude and longitude) (PC2: 21%). Thus, the null hypothesis of no environmental pattern among stations was rejected.

Total chlorophyll *a* concentration was highest in the T-bloom group of stations, with some extension into a few stations at the edges of the pre-bloom and C-bloom groups (i.e. June stations 7, 14, 27, and 31) (Online Resource 5). In general, high chlorophyll *a* concentration was coincident with intermediate temperatures and nutrient concentrations, over a wide range of salinities. Moderate chlorophyll *a* concentration was relatively extensive in time (PC1) and space (PC2) over the NOW, characteristic of the prolonged bloom of *C. socialis*. As shall be seen below, most of the stations with abundant oikopleurid and fritillarid appendicularians were in the upper left quadrant of Online Resource 5, at moderate, C-bloom concentrations of chlorophyll *a*.

Phenology of abundance and biomass of appendicularians

During April and May, the abundance of *O. vanhoeffeni* was generally low, with highest values along the Ellesmere Island shore of the central NOW at stations 22, near the mouth of Smith Bay, and 44, near the mouth of Jones Sound and the Jones Sound polynya, north-east of Coburg Island (Fig. 3a). Abundance was much lower at the remaining stations, although *O. vanhoeffeni* was present throughout the area sampled, including at stations 2 and 7 in the northern extremity of the study area.

The biomass of *O. vanhoeffeni*, which reflects the relative abundance of larger animals, had a somewhat different distribution in April and May than did abundance. Biomass was highest at central stations along both the east and west margins of the central NOW, especially station 40, near the mouth of Inglefield Bay and the Inglefield Bay polynya, and station 44, in the Jones Sound polynya (Fig. 4a). Biomass was low at the remaining stations sampled, including station 22, which had the second highest abundance in May (Fig. 3a).

Peak abundance of *O. vanhoeffeni* increased by ca. an order of magnitude in June, with high concentration at station 54 in the south-eastern-central NOW, near Greenland (Fig. 3b). On the western side of the NOW, the more moderate abundances were ca. twofold and tenfold higher than in April–May, at stations 22 and 44, respectively. Abundances remained low at northern and southern stations.

Biomass of *O. vanhoeffeni* in June was fivefold to tenfold higher at a few stations in the central NOW in comparison with April–May (Fig. 4b). Largest biomass occurred at stations 22 and 31 in the western-central NOW near the mouth of Smith Bay (14–29 mg C m^{-2}), although these stations did not have the most abundant populations in June (Fig. 3b). Station 54, in the eastern-central NOW, had the highest abundance of the stations sampled in June, but a relatively low biomass (Fig. 4b). All the other stations sampled had low biomass values.

Of the 8 stations sampled during July, only stations in the central NOW had moderate or high abundances of *O. vanhoeffeni* (Fig. 3c). Peak abundance (ca. 10,300 m^{-2} at station 44) was ca. twofold greater than in June, with greatest abundances once again on both the eastern and western sides of the NOW, at stations 40 and 44, respectively, near the mouths of Inglefield Bay and Jones Sound. Abundances were moderate at deeper stations along the central NOW channel (i.e. stations 35 and 54).

Biomass of *O. vanhoeffeni* in July again displayed a different spatial pattern than did abundance (Fig. 4c). Biomass was high in the central NOW at station 35, about fourfold greater than peak biomass values for any of the stations sampled in June (Fig. 4b). For the first time, moderate biomass was observed at northern stations (2 and 5) in Smith Sound.

All 14 stations visited in September, including southern and northern stations, had moderate or high abundances of *O. vanhoeffeni* (Fig. 3d). Peak abundances were ca. twofold greater than in July and ca. 75-fold greater than in April–May. Abundance was generally lower along the western side of the NOW, except at the most southerly station, 66 (Fig. 3c).

In contrast to previous months, stations with highest biomass of *O. vanhoeffeni* in September were all in the northern NOW (Fig. 4d). Maximum biomass at station 14 (240 mg C m^{-2}) was ca. twofold greater than maximum biomass in July at station 35 (Fig. 4c) and almost 2 orders of magnitude greater than maximum biomass values in April–May in the central NOW (Fig. 3a). Moderate biomass was observed at all remaining stations. In the southern NOW (i.e. stations 66, 68, and 76), biomass values were several orders of magnitude greater than in any previous month.

Fritillaria borealis lagged *O. vanhoeffeni* in seasonal population growth. There were essentially no *F. borealis* at any of the stations sampled in April and May (data not shown). In June, peak abundances were in the central NOW, at stations 44 and 54 (Fig. 5a), as was the case for *O. vanhoeffeni* during June (Fig. 3b). Abundance was low at all the other stations sampled in June. Biomass of *F. borealis* was very low in June (data not shown).

Fig. 3 North Water oikopleurid appendicularians. Abundance (m^{-2}) maps of *Oikopleura vanhoeffeni* for those stations with tows to at least 100 m depth. Abundance is proportional to the area of the bubbles. Station numbers appear below the bubbles in most cases or as near the bubbles as possible when necessary. Each bubble is centred on a station location. The 500-m bathymetric contour is shown by a *dotted line*. **a**: April and May; **b** June; **c** July; **d** September
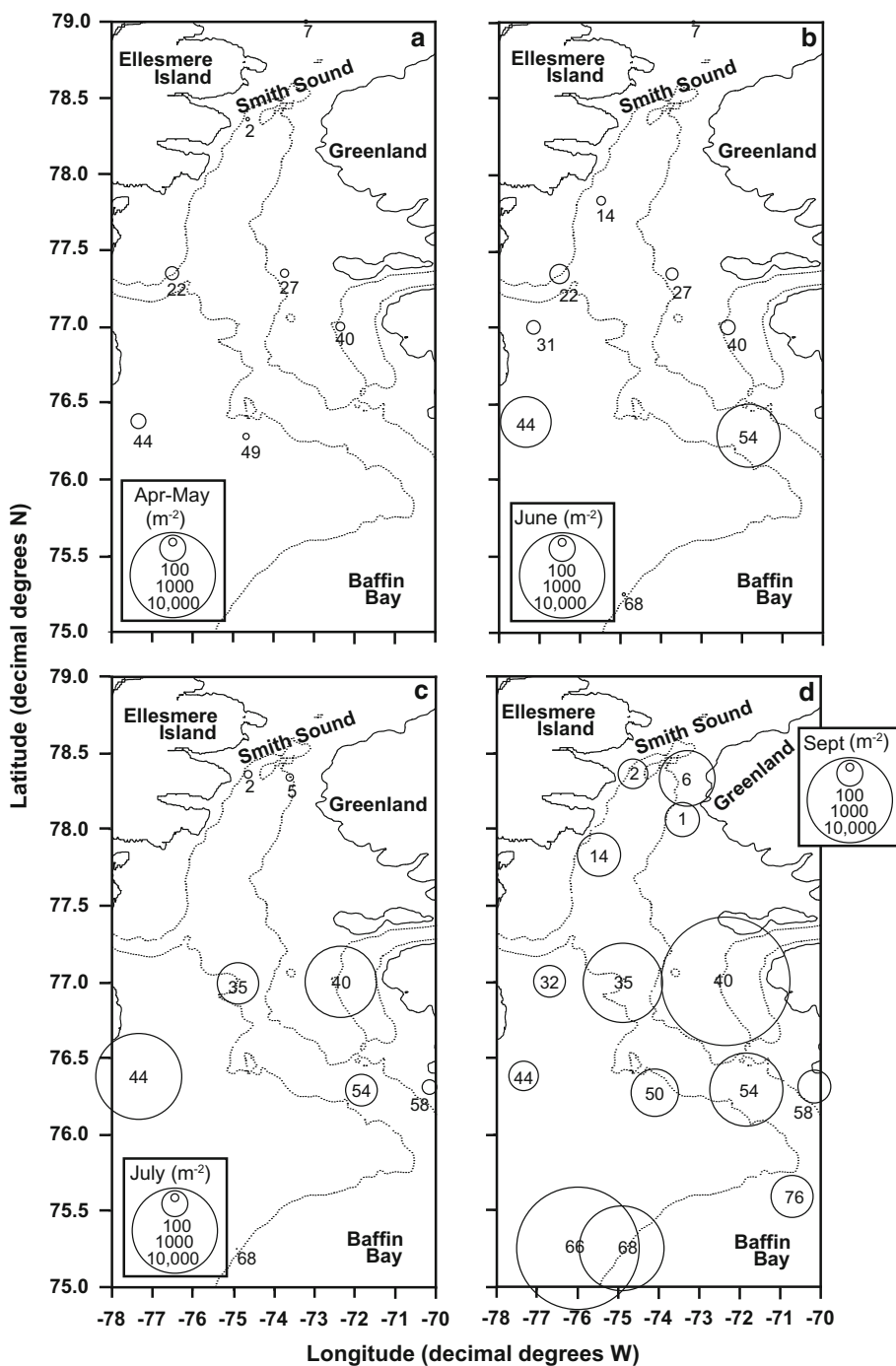

Peak abundance of *F. borealis* increased <twofold in July. This increase was concentrated in the central NOW (Fig. 5b), though biomass was still low. All remaining stations had low biomass values.

Fritillaria borealis abundance increased by more than an order of magnitude between July and September, reaching peak values for the entire study (e.g. >53,000 animals m^{-2} at station 2) (Fig. 5c). Abundance and biomass of fritillarids were generally greater in the northern

NOW and along the Ellesmere Island coast (e.g. stations 2, 14, and 32). *F. borealis* biomass was moderate to high north of 76.5°N, with a maximum value of 5 mg C m^{-2} at station 2. Abundance and biomass values were generally lower in the southern and eastern NOW. Biomass values at stations south of 76.5°N were moderate to low.

The abundance of *O. vanhoeffeni* increased exponentially after mid-April, while that of *F. borealis* increased exponentially after the second week of June (Fig. 6).

Fig. 4 North Water oikopleurid appendicularians. Biomass (mg carbon m^{-2}) maps of *Oikopleura vanhoeffeni* for those stations with tows to at least 100 m depth. For explanation of *symbols* and *numbers*, see legend for Fig. 3
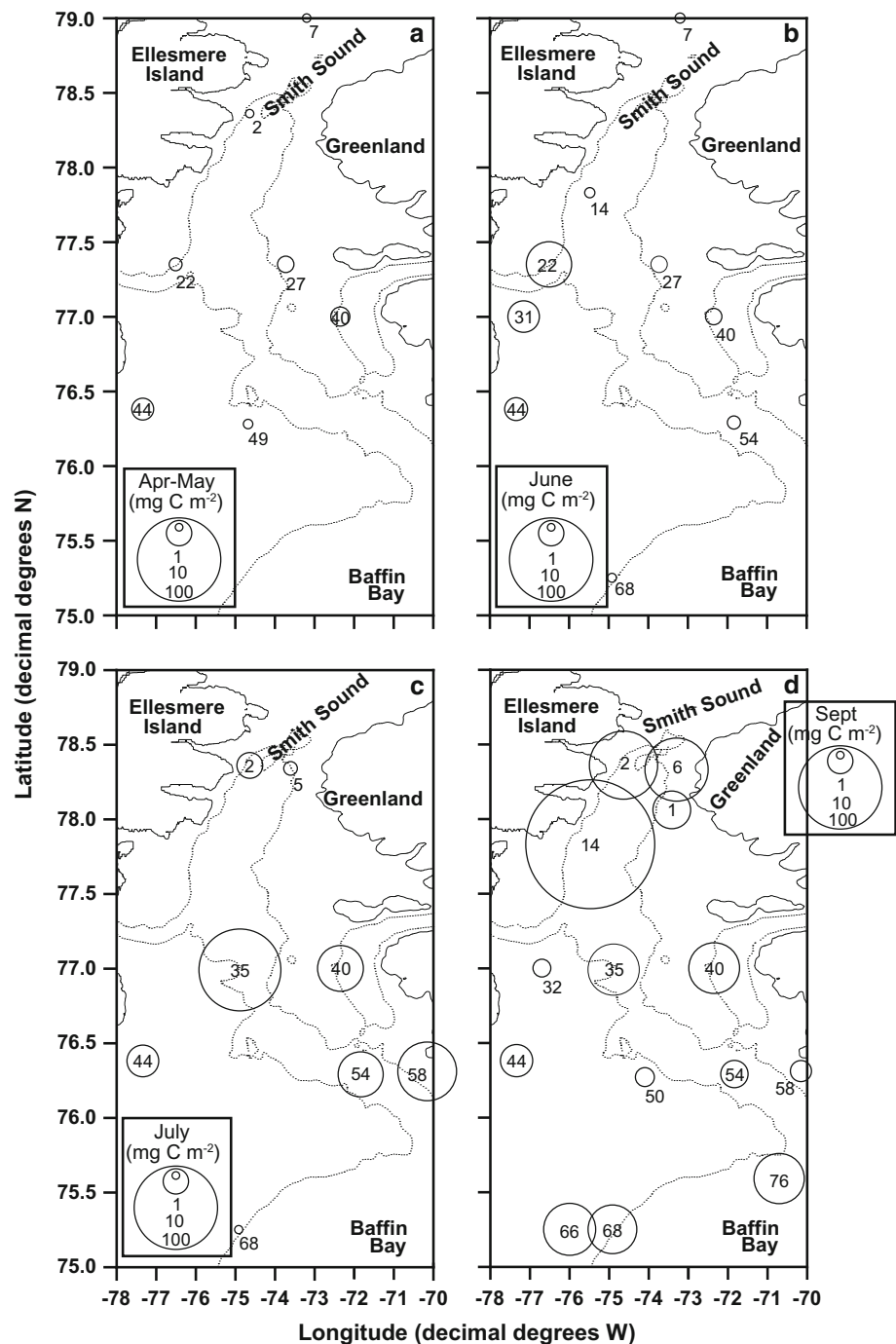
Phenology of spawning of *Oikopleura vanhoeffeni*

There were regional differences in the phenology of spawning by *O. vanhoeffeni* in the NOW. Pre-spawning populations were essentially unimodal, predominately maturity stage IV and V. Spawning populations had bimodal maturity stage distributions, with maturity stage I forming the younger mode and stages IV and V the older mode. Trunk length of spawning populations was

distributed evenly across many size categories. Post-spawning populations had essentially unimodal trunk length and maturity stage distributions, dominated by small animals with trunk lengths from 0.3 to 1.0 mm and maturity stages I and II. Over the entire NOW area, spawning occurred from April through September, beginning in late April at station 49 in the south-central NOW. Spawning began from mid-June to mid-July at other central stations, from mid-June to September at northern stations, and
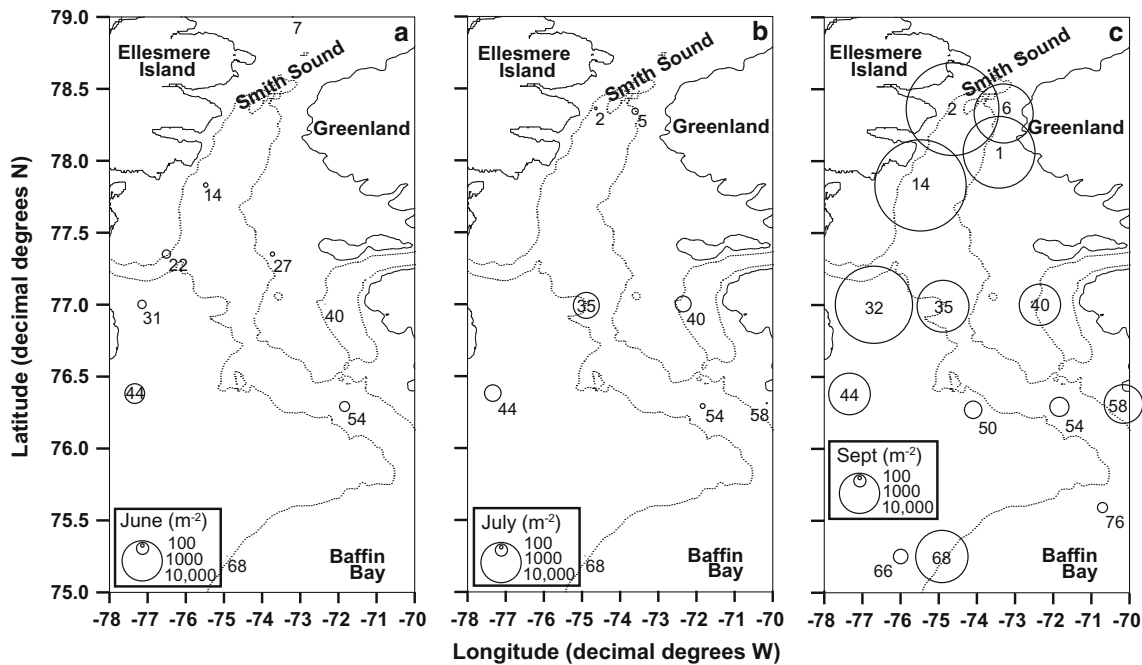
Fig. 5 North Water fritillarid appendicularians. Abundance (m^{-2}) maps of *Fritillaria borealis* for those stations with tows to at least 100 m depth. Since biomass of *F. borealis* was estimated by multiplication of abundance by a constant (see "Methods"), the maps of biomass have an identical pattern to these of abundance. **a** June; **b** July; **c** September. There were no *F. borealis* in the net-tow samples in April–May. For explanation of *symbols* and *numbers*, see legend for Fig. 3
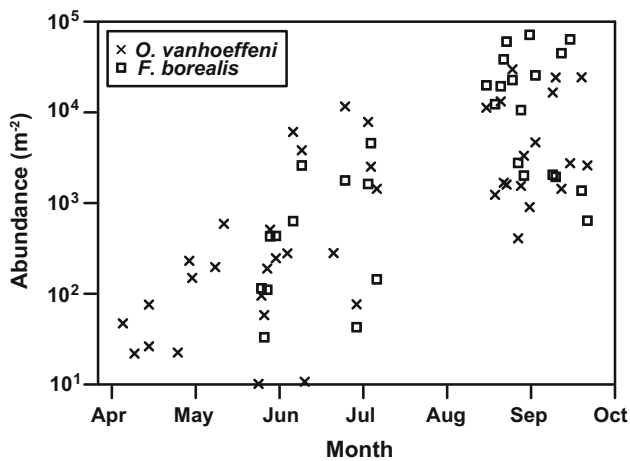

Fig. 6 North Water appendicularians. Log$_{10}$ of the abundance (m^{-2}) of *Oikopleura vanhoeffeni* (*cross*) and *Fritillaria borealis* (*open square*) versus day of the year for those stations with tows to at least 100 m depth

finally at two southern stations in late September. Interpretation of time series data from specific stations or sets of stations is potentially confounded by surface water advection. In general, a spawning duration of ca. 2–3 months was observed at two east-central stations *versus* ca. one month in the rest of the NOW.

There was evidence of recent spawning at station 49 in late April (Fig. 7a), under moderate ice cover. However,

the population at Station 40 (77.0°N) was in a pre-spawning state in early May (data not shown) and again when sampled in late May (Fig. 7b). There were no population data for the other stations sampled in April and May (i.e. stations 2, 7, 22, 27, and 44).

Populations spawned at stations 31 and 22 in mid-June, in the western-central NOW (Fig. 7c). The population at station 14 in the northern NOW was in a pre-spawning state (data not shown), while that at station 18 had recently spawned (Fig. 7d). All four of the above stations had moderate-to-high concentrations of *Thalassiosira* spp. in June (Booth et al. 2002). Station 44 in the central NOW near the mouth of Jones Sound also had recently spawned (data not shown). There were no population data for the other stations sampled in June (i.e. 7, 27, 40, 54, and 68).

There was evidence of spawning at station 54 in the eastern-central NOW in July, but high abundances in June (Fig. 3b) suggest that spawning also had occurred previously at station 54 in May or early June. There was no evidence of populations in a pre-spawning state in July. The populations at stations 1, 35, 40, and 44 had recently spawned, station 40 perhaps more recently than station 35 (Fig. 7e, f). There were no population data for the other stations sampled in July (i.e. 2, 58, and 68).

The first evidence of spawning in the southern NOW occurred at stations 66 and 76 in late September. There was no evidence of populations in a pre-spawning state in

Fig. 7 North Water oikopleurid populations. Relative frequency distributions of trunk length (mm, in 1.0 mm length classes) and maturity stage (after Shiga 1976) of *Oikopleura vanhoeffeni* at stations representing pre-bloom (**a–c**), T-bloom (**d**), and C-bloom (**e–h**) groups. **a** Station 49, 23 April; **b** station 40, 25 May; **c** station 22, 13 June; **d** station 18, 11 June; **e** station 35, 18 July; **f** station 40, 17 July; **g** station 2, 11 September; **h** station 40, 20 September. All samples came from surface tows within the upper 100 m except (**b**), which came from 0 to 150 m
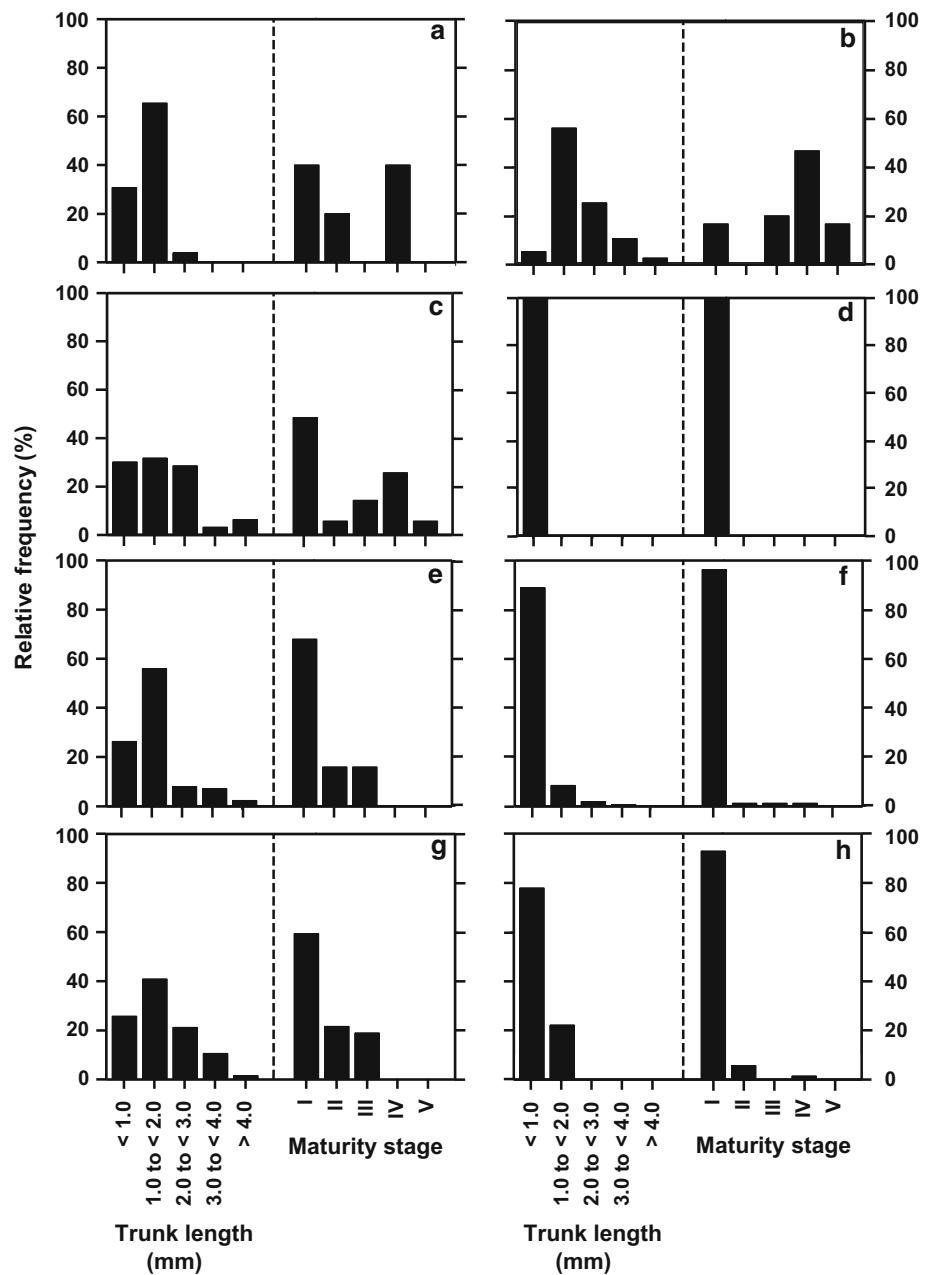
September. The populations at stations throughout the rest of the NOW had recently spawned, including stations 1, 2 (Fig. 7g), 6, and 14 (north); 32, 35, 40 (Fig. 7h), 50, 54, and 58 (central); and 68 (south). There were no population data for station 44 in September.

Apparently, more than one generation of *O. vanhoeffeni* occurred during the study period at stations 40 and 54. Alternatively, advection may have supplied ready-to-spawn animals over a longer period than for other stations. The population at station 40 was in a pre-spawning state in May (Fig. 7b), and abundance remained low in June (Fig. 3b). In July, the population was in a post-spawning state (Fig. 7f), and abundance was much higher (Fig. 3c).

Thus, the population at station 40 must have spawned between mid-June and July. Two samples from station 40 in September also indicated a post-spawning population (Fig. 7h, 20 September). All three July and September post-spawning populations included large fractions of small (78–90% <1 mm trunk length), immature (93–96% maturity stage I) individuals, suggesting essentially continuous recruitment from July to September. Since abundance at station 40 peaked in September (25×10^3 m^{-2}) (Fig. 3d), at least one generation followed that produced between mid-June and July.

Similarly, the population of *O. vanhoeffeni* at station 54 was spawning in July (Fig. 8a) and was in a post-spawning
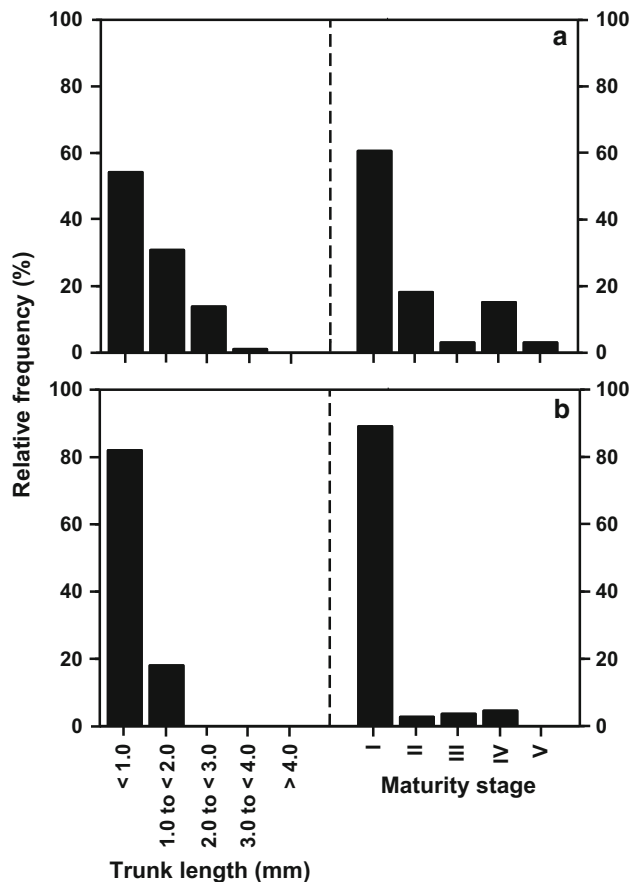
Fig. 8 North Water oikopleurid populations. Relative frequency distributions of trunk length (mm, in 1.0 mm length classes) and maturity stage (after Shiga 1976) of *Oikopleura vanhoeffeni* at station 54 on 20 July (**a**) and 19 September (**b**)

state in late September (Fig. 8b), when abundance was highest (14×10^3 m^{-2}) (Fig. 3d), but biomass was very low (Fig. 4d). The late-September maximum abundance was preceded by more moderate numbers in July (Fig. 3c) and early September. Although there are no maturity stage data available to show spawning at station 54 before July, high late-June abundance (5.5×10^3 m^{-2}) (Fig. 3b) and biomass (Fig. 4b) suggest spawning in June, as well as in September (i.e. there was high abundance and low biomass in both June and September). All animals collected at station 54 in June were <1 mm long (data not shown), consistent with recent spawning.

Hypotheses concerning associations between appendicularian abundance, biomass, and environmental pattern

The abundance of *O. vanhoeffeni* was strongly, positively associated with oikopleurid biomass, and both abundance and biomass were significantly and similarly (i.e. similar sign) associated with the six environmental variables which

defined the temporal and spatial pattern of the environment (Table 2; Fig. 2). There was no association between abundance or biomass and the euphotic zone concentration of chlorophyll *a*. Abundance and biomass increased with increasing temperature and with decreasing salinity, density, silicate concentration, and euphotic zone depth, all characteristic of advancing season (i.e. time). The effect strength of temperature was strongest of all environmental variables for the abundance of *O. vanhoeffeni*. The effect strength of temperature was moderate for the biomass of *O. vanhoeffeni*, as were all the other environmental variables (Table 2).

Since the abundance of *F. borealis* was strongly, positively associated with both the abundance and biomass of *O. vanhoeffeni*, *F. borealis* abundance had similar associations with environmental variables as did *O. vanhoeffeni* abundance, in both magnitude and sign (Table 2). The effect strength of euphotic zone salinity and surface density on the abundance of *F. borealis* was greater than for the abundance and biomass of *O. vanhoeffeni*.

The abundance of *O. vanhoeffeni* was low at most of the stations in the pre-bloom and T-bloom groups (Fig. 9a). Stations 22 and 44, in the western-central NOW, had highest abundances. These stations were in the middle of the pre-bloom group, indicating slight warming and lower nutrient concentrations at the beginning of the phytoplankton bloom. Station 76, in the T-bloom group, had moderate abundance, but this station occurred in September at relatively high temperatures and low nutrient concentrations, indicating a waning bloom of *Thalassiosira* spp. in the south-eastern NOW at that time. In fact, Booth et al. (2002) found the phytoplankton at station 76 in September to be dominated by *C. socialis*. Abundance was moderate or high at many stations in the C-bloom group, particularly at central and southern stations (Fig. 9a). Although the stations with high abundance were all south of 77.5°N, these stations were observed in all water masses (i.e. high abundances were spread over a wide range of PC2 values). Thus, the abundance of oikopleurid appendicularians was primarily a seasonally dependent (i.e. variability along PC1), rather than a spatially dependent (i.e. variability along PC2), phenomenon. This observation was further supported by the relationship between the abundance of *O. vanhoeffeni* and the PC scores of the stations, which was highly significant (with negative sign) for PC1 scores (i.e. time), but not significant for PC2 scores (space) (Table 3).

Oikopleura vanhoeffeni biomass, reflecting populations dominated by large, pre-spawning animals, was low or moderate at most pre-bloom and T-bloom stations, except for two stations in the pre-bloom group (i.e. 44 and 22, occupied in May and June, respectively, and dominated by SRAW), and two stations in the T-bloom group (i.e. 40 and

Table 2 Spearman's rank–order correlation coefficients (rho) among the abundance and biomass of *Oikopleura vanhoeffeni*, *Fritillaria borealis*, and the best six environmental covariates with, in addition, chlorophyll *a* concentration integrated over the euphotic zone

	Oikabund (m^{-2})	Oikmass (mg C m^{-2})	Fritabund (m^{-2})	Temp$_{100}$ (°C)	Salinity$_{euph}$	Sigma-t_{surf} (kg m^{-3})	Silicate$_{uml}$ (mmoles m^{-2})	Silicate$_{100}$ (mmoles m^{-2})	Euphotic zone depth (m)	chl a_{euph} (mg m^{-2})
Oikabund	1	0.78***	0.76***	0.76***	−0.50***	−0.48***	−0.68***	−0.40**	−0.34*	NS
Oikmass		1	0.71***	0.52***	−0.52***	−0.50***	−0.55***	−0.30*	−0.47***	NS
Fritabund			1	0.68***	−0.79***	−0.74***	−0.50***	NS	−0.39**	NS

Abundance and biomass were integrated over ≥100 m. * = $p < 0.05$, ** = $p < 0.01$, *** = $p < 0.001$. Values of rho not significantly different from 0 at $p > 0.05$ are indicated by 'NS'. $n = 46$ for all comparisons

'Oikabund' = abundance of *Oikopleura vanhoeffeni*; 'Oikmass' = the biomass of *Oikopleura vanhoeffeni*; 'Fritabund' = the abundance of *Fritillaria borealis*; 'Temp$_{100}$' = the mean water temperature of the upper 100 m; 'Salinity$_{euph}$' = the mean salinity of the euphotic zone; 'Sigma-t_{surf}' = the sea water density at 5 m depth; 'Silicate$_{uml}$' = the silicate concentration integrated over the upper mixed layer; 'Silicate$_{100}$' = the silicate concentration integrated over the upper 100 m; 'chl a_{euph}' = the concentration of chlorophyll *a* equivalents in the total seston integrated over the euphotic zone

76, occupied in May and September, respectively, and dominated by BBW) (Figs. 9b, 2b). Highest biomass overall occurred at stations 14 and 2 in the C-bloom group in September, dominated by a mixture of BBW and SRAW, with BBW predominant (Fig. 2b). As was the case for abundance, the biomass of *O. vanhoeffeni* had a strong, negative association with PC1 scores, but no relationship with PC2 scores (Table 3).

Fritillaria borealis abundance and biomass were very low at stations in the pre-bloom and T-bloom groups and high only at several stations in the C-bloom group (Fig. 9c). Ten of the 11 stations with highest abundance and biomass were sampled in September (Fig. 2a). Although eight of these 11 stations were on the western side of the NOW, nine of 11 were in BBW, which covered most of the NOW in September (Fig. 2b). As with *O. vanhoeffeni*, *F. borealis* abundance was highly associated (negative sign) with station scores on PC1 (i.e. time) (Table 3). However, unlike *O. vanhoeffeni*, there was a weak-to-moderate, significant, positive association of fritillarid abundance with PC2 scores (i.e. space), supporting the observation of a preponderance of stations with high abundance along the Ellesmere Island shore of the NOW (i.e. western sector), with relatively high temperatures and low salinities late in the season (i.e. the upper left quadrant of Fig. 9c).

The high relative frequency of small, recently produced *O. vanhoeffeni* of maturity stage I indicated recent or ongoing spawning at almost all the C-bloom stations and at 5 of the 9 stations in the pre-bloom and T-bloom groups (Fig. 10a; the relative frequency of maturity stage I had a similar pattern and is not shown). This pattern was statistically supported by moderately strong, negative associations between the relative frequency of *O. vanhoeffeni* <1 mm long and of maturity stage I, with the station

scores on PC axis 1 (Table 3). However, there were no significant associations between the relative frequencies of small, immature stage I animals and the station scores on PC axis 2 (Table 3), indicating lack of a coherent pattern of small, immature animals in space (Fig. 10a).

The high relative frequency of mature, pre-spawning *O. vanhoeffeni* of maturity stages IV and V, along with a high abundance of small animals, indicated that spawning was ongoing at the time of sampling at ca. 12 of the 21 stations in the C-bloom group (Fig. 10b). Since the remaining stations had a high abundance of small animals and lower relative abundance of large, pre-spawning animals, spawning must have occurred within less than a few weeks before sampling. Four of the 5 stations in the pre-bloom and T-bloom groups, for which maturity stage data were available, had relative frequencies of mature, pre-spawning *O. vanhoeffeni* >25%, indicating a readiness to spawn (Fig. 10b). There was a moderately strong, positive association between the relative frequency of maturity stage IV animals and the station scores on PC1, and a weak negative relationship with the PC2 scores (Table 3). This pattern indicates predominance of maturity stage IV early in the season in relatively cold, nutrient-rich BBW, predominantly in the lower right quadrant of Fig. 10b. A stronger negative relationship occurred between the relative frequency of maturity stage V *O. vanhoeffeni* and the station scores on PC2, indicating predominance of this life history stage in the lower half of the PC plot (Fig. 10b), generally coinciding with stations with higher chlorophyll *a* concentration (Online Resource 5).

The largest size class of *O. vanhoeffeni* (>4 mm long) had positive associations with station scores on both PC 1 and PC 2 axes, indicating that large animals in surface samples were predominantly found at lower water temperatures from April to June, but also in samples collected

Fig. 9 North Water appendicularian populations versus environmental pattern. Bubble plots of appendicularian abundance (m^{-2}) and biomass (mg carbon m^{-2}) on the environmental principal component axes PC1 and PC2, from Fig. 2. **a** Abundance of *Oikopleura vanhoeffeni*; **b** biomass of *O. vanhoeffeni*; **c** abundance of *Fritillaria borealis*. Data are shown for those stations having tows to at least 100 m depth. Station *number* is shown at the centre of each bubble except when the bubble is too small or bubbles overlap, when the station *number* is shown immediately adjacent to the bubble
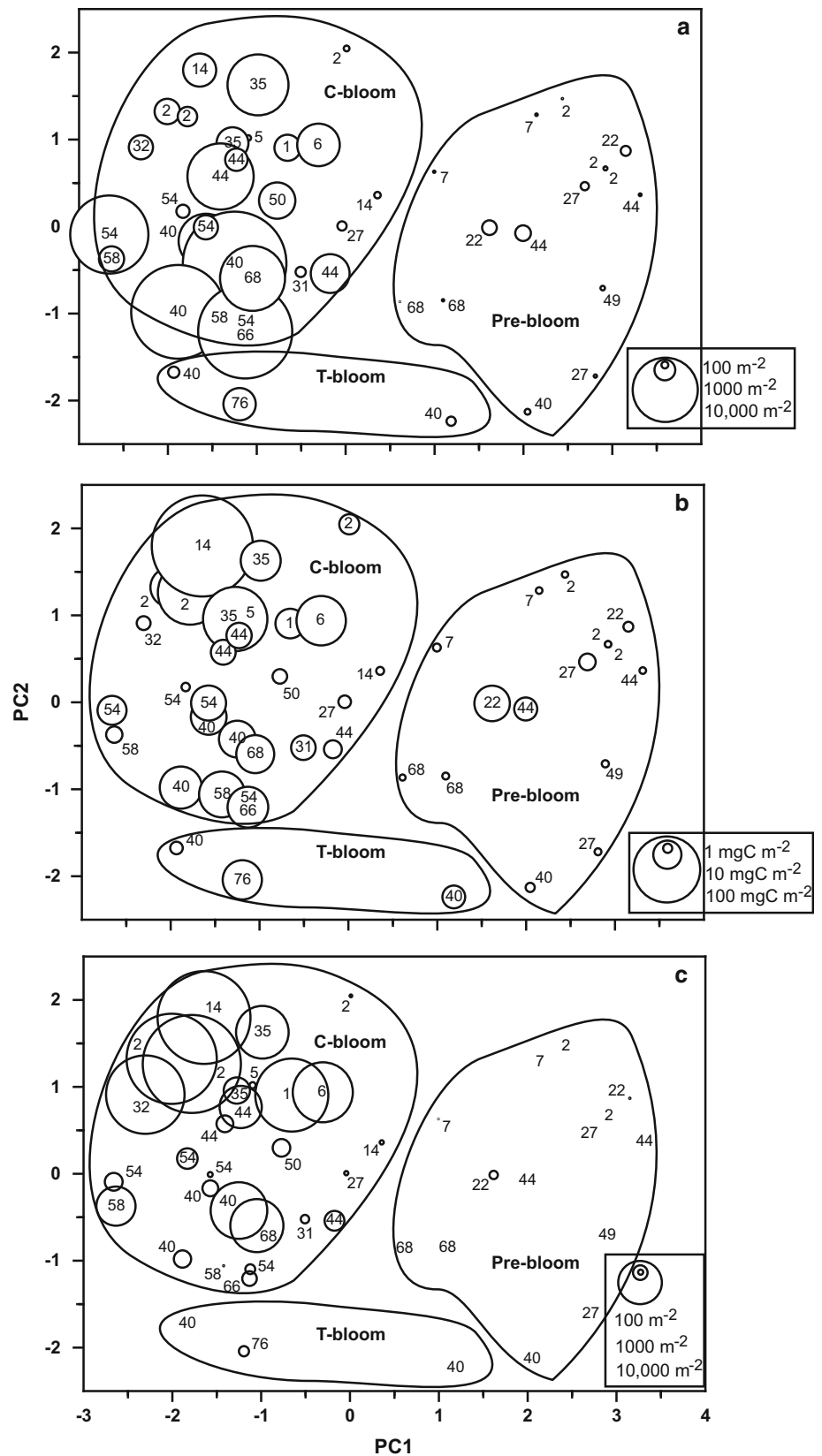
Table 3 Spearman's rank–order correlations (rho) between the abundance and biomass of *Oikopleura vanhoeffeni*, *Fritillaria borealis,* and demographic (i.e. trunk length frequencies) (mm), and life history (i.e. maturity stage frequencies) (I–V) variables of *O. vanhoeffeni* from net-tow samples, and the station scores on principal component axes 1 and 2 from ordination of the environmental data (see Fig. 2a, b)

Population variate	Station score on pc axis 1	Station score on pc axis 2	n
Oikabundance	-0.67^{***}	NS	46
Oikmass	-0.62^{***}	NS	46
Fritabundance	-0.72^{***}	0.33^{*}	46
<1 mm$_{all}$	-0.36^{**}	NS	60
<1 mm$_{<100}$	-0.42^{**}	NS	37
$1–2$ mm$_{all}$	0.30^{*}	NS	60
$1–2$ mm$_{<100}$	0.37^{*}	NS	37
$2–3$ mm$_{all}$	0.29^{*}	NS	60
>4 mm$_{all}$	NS	0.26^{*}	60
>4 mm$_{<100}$	0.33^{*}	NS	37
>4 mm$_{>100}$	NS	0.61^{**}	22
Maturity I$_{all}$	-0.32^{*}	NS	40
Maturity IV$_{all}$	0.45^{**}	-0.31^{*}	40
Maturity IV$_{<100}$	0.49^{*}	NS	25
Maturity V$_{<100}$	NS	-0.42^{*}	25

$* =$ rho significantly different from 0 at $p < 0.05$; $**$ at $p < 0.01$, and $***$ at $p < 0.001$. Those trunk length and maturity stage classes not shown had no significant values of rho at $p < 0.05$ on either pc axis

Subscript 'all' indicates that all tows available at a given station were used, regardless of depths covered. Subscript '<100' indicates that only those tows in the upper 100 m were used for the analysis, and subscript '>100' indicates that only those tows at depths >100 m were used in the analysis. $n =$ the number of tows used for the analyses in each row of the table

from >100 m in the north-central and northern NOW after June (Table 3). Immature *O. vanhoeffeni* with body sizes from 1 to 2, 2 to 3, and >4 mm from the surface samples had similar, positive associations with the station scores on the PC 1 axis, i.e. at colder water temperatures earlier in the season (Table 3).

Discussion

The objective of this paper was to further understand the spatial pattern of population phenology of appendicularians over an entire productive season in the NOW. *Oikopleura vanhoeffeni* is a cryophilic, stenohaline appendicularian (Choe and Deibel 2008), capable of ingesting a wide size range of food, from colloids to diatoms >30 μm in size (Flood et al. 1992; Acuña et al. 1996). This species has a circum-Arctic distribution and is common and abundant in the boreal north Pacific and Atlantic oceans (Shiga 1993; Shiga et al. 1998; Choe and Deibel 2008). *Oikopleura vanhoeffeni* consumes a substantial portion of primary production and is a major secondary producer, in both the Northeast Water Polynya (Acuña et al. 1999), and in Conception Bay, Newfoundland (Choe and Deibel 2011), which is influenced by the inshore branch of the Labrador Current.

Due to the high latitude and cold-water temperatures of the NOW, most, and perhaps all, of the oikopleurid specimens collected were *O. vanhoeffeni*. For example, only Dvoretsky and Dvoretsky (2009) have reported *O. labradoriensis* from high latitudes in the northern hemisphere, in 'Atlantic Water' in the Barents and Pechora seas, at minimum water temperatures >2.0 °C. Depth-specific temperatures >2.0 °C were observed at only three stations in the south-central and southern NOW in July and September (i.e. stations 44, 54, and 68), all at depths <16 m. Given the limited thermal habitat available for *O. labradoriensis* in the NOW during our study, all the oikopleurid appendicularians collected were assumed to be *O. vanhoeffeni*.

Fritillaria borealis is an eurythermal and euryhaline appendicularian (Choe and Deibel 2008), often abundant in coastal waters with lower than oceanic salinities (Wyatt 1973; Dvoretsky and Dvoretsky 2009). This species has a broad distribution in the northern hemisphere, from temperate to polar waters (Fenaux et al. 1998). *Fritillaria borealis* consumes a similar size range of particles as do oikopleurids, with ca. 80% of the diet coming from particles <15 μm in size (Flood 2003; Fernández et al. 2004). Due to consumption of very small, abundant particles, the abundance of *F. borealis* may be regulated by predators rather than by food availability (Skjoldal et al. 1993). Because of a small body size, this fritillarid is often the most abundant appendicularian in zooplankton samples (Choe and Deibel 2008; Dvoretsky and Dvoretsky 2009, 2013).

Fig. 10 North Water oikopleurid populations versus environmental pattern. **a** Bubble plot of the tow-wise (surface stratum only) relative frequency (%) of small *Oikopleura vanhoeffeni*, with a trunk length <1 mm, on the environmental principal component axes PC1 and PC2, from Fig. 2. **b** Similar bubble plot for pre-spawning, adult *O. vanhoeffeni* of maturity stages IV and V. For explanation of *numbers* and *symbols*, see the legend for Fig. 9
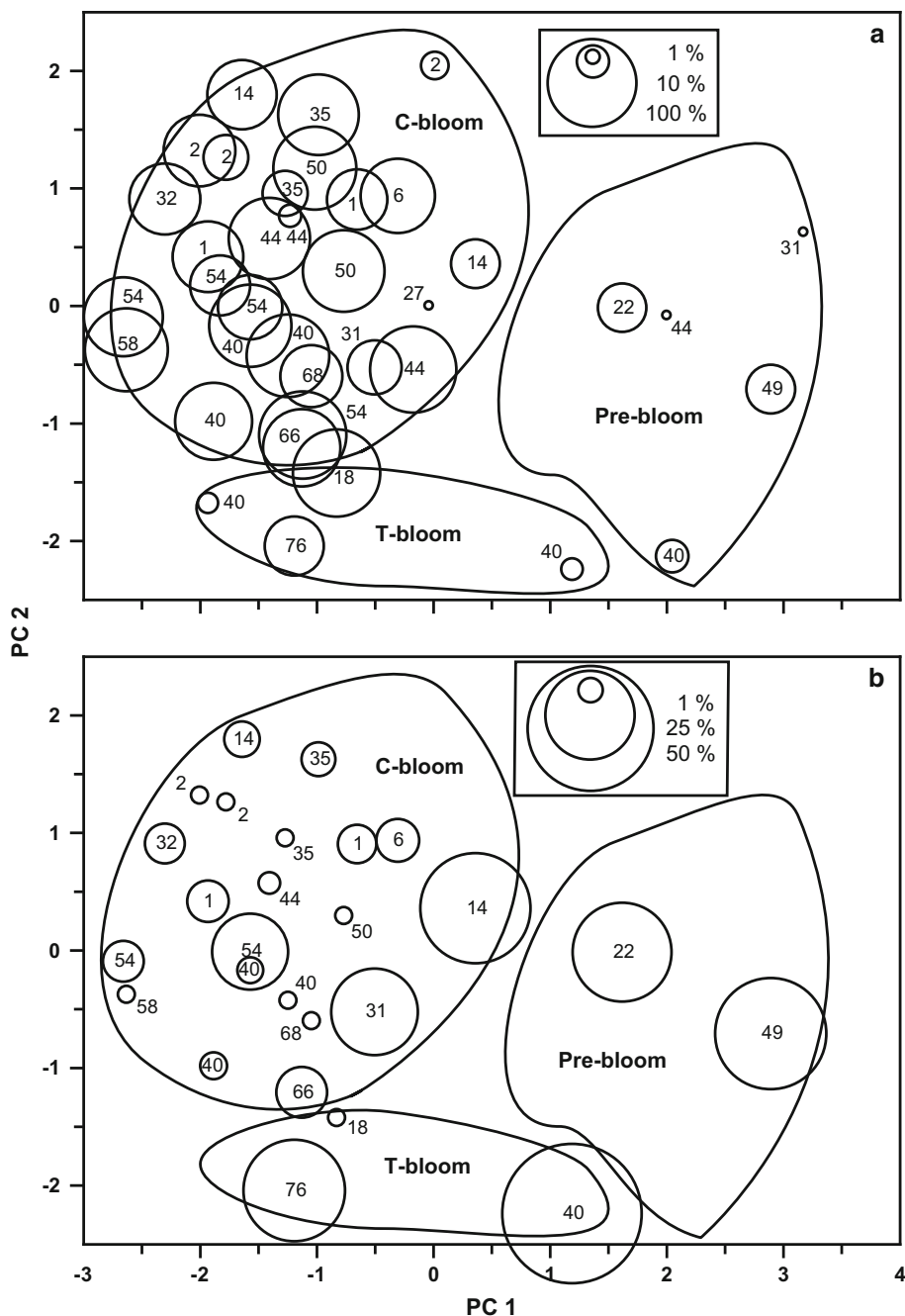
When and where do appendicularians spawn in the NOW?

Seasonal cycles of appendicularian populations have long been known in non-polar waters (Fenaux 1961, 1976; Acuña and Anadón 1992; Acuña et al. 1995). In north-temperate waters, fritillarids generally occur first in the annual sequence, predominating in low-salinity water during winter. Several species of oikopleurids may follow in succession during spring and summer, as the upper mixed layer becomes warmer and more saline. This

temperate successional sequence seems to be inverted in the NOW, perhaps due to the seasonal cycle of sea ice formation and melting, with lowest salinities in the upper mixed layer occurring in late summer and autumn, rather than in late winter and spring.

Earliest spawning of *O. vanhoeffeni* begins in synchrony with the early bloom of diatoms (i.e. the *Thalassiosira* bloom, or 'T-bloom') in April and May at central stations across the breadth of the NOW. In May, abundance and biomass of *O. vanhoeffeni* are highest at station 44, located in or near the Jones Sound polynya, suggesting early,

ongoing spawning in the west-central NOW. The Jones Sound polynya is known to be productive during early spring and is a hotspot for zooplankton, Arctic cod (*Boreogadus saida*), and marine mammals, including walrus (*Odobenus rosmarus*), beluga (*Delphinapterus leucas*), ringed seals (*Phoca hispida*), bowhead whales (*Balaena mysticetus*), and narwhals (*Monodon monoceros*) (Richard et al. 1998a; Thiemann et al. 2007; Stewart 2008). For example, walrus and beluga are known to overwinter from February to May in polynyas at the mouths of Jones Sound and Inglefield Bay, both members of the NOW system of polynyas (Richard et al. 1998b; Tang et al. 2004; Stewart 2008). Sometimes the Jones Sound polynya is bifurcated, with one arm west of Coburg Island and another north-east of Coburg Island and south-east of Clarence Head, Ellesmere Island (see Fig. 1 in Richard et al. 1998a), near station 44. The biomass of *O. vanhoeffeni* and concentration of chlorophyll *a* are also elevated in May at station 27 in the east-central NOW, indicating gonad maturation and imminent spawning in response to phytoplankton abundance near the Inglefield Bay polynya.

Although station 44 in the western NOW had the highest abundance and biomass of *O. vanhoeffeni* in May, along with increasing concentration of chlorophyll *a*, station 22, ca. 50 km north of station 44, had moderate abundance but low biomass in May, indicating spawning sometime in late April. The first evidence of spawning in the eastern NOW was also in May, at station 40 near the mouth of Inglefield Bay, along with a relatively high concentration of chlorophyll *a*. Thus, the early appearance of *O. vanhoeffeni* at stations 40 and 44 is likely due to the presence of polynyas at the mouths of Jones Sound and Inglefield Bay, on the western and eastern sides of the central NOW, respectively (see Fig. 1 in Richard et al. 1998a).

In subsequent months, spawning and population growth of *O. vanhoeffeni* follow the progression of open water and the summer blooming of *C. socialis* (i.e. the 'C-bloom'), northwards and southwards from the south-central NOW. Highest abundances remain in the south-central NOW throughout the June–September period, spatially associated with relatively high concentrations of chlorophyll *a* near the mouths of Jones Sound and Inglefield Bay. Abundance and biomass are high in the northern NOW near the Smith Sound polynya (i.e. >77.5°N) only in September, likely in association with the relatively late, high productivity of *C. socialis* (Booth et al. 2002). Abundance and biomass of *O. vanhoeffeni* increase by about two orders of magnitude from April to September, equivalent to a population growth rate of ca. 0.03 day^{-1}, or a numerical doubling time of ca. 23 days. This population growth rate is high for a multicellular metazoan at near-zero water temperatures and 77°N latitude. For example, the median population growth rate of *O. vanhoeffeni* from April to September in Conception Bay, Newfoundland, at 47°N, is ca. 0.008 day^{-1} (Choe and Deibel 2011), equivalent to a numerical doubling time of ca. 86 day.

There are several lines of evidence indicating that *O. vanhoeffeni* was consuming diatoms in the NOW during this study, despite the large size of many of the prey species during the T-bloom, and the formation of colonies by *C. socialis* during the C-bloom. Acuña et al. (2002) found that gut chlorophyll content increased in NOW *O. vanhoeffeni* up to a chlorophyll *a* concentration of 250 mg m^{-2} (ca. 5 μg chl *a* l^{-1}). This functional response demonstrates the ability of *O. vanhoeffeni* to feed at relatively high concentrations of large diatoms. In fact, for much of July and September, the population grazing rate of *O. vanhoeffeni* was approximately equal to that of all the copepod species combined, and oikopleurid population grazing accounted for a high proportion of total phaeopigments in the water column (Acuña et al. 2002; Deibel et al. 2005). Microscopic analyses of faecal pellets collected in July showed 49 to ca. 100% diatom content, with a median of 25% *C. socialis* and 20% *Thalassiosira bioculata* (Acuña et al. 2002). In total, 89% of the faecal pellets examined contained *C. socialis* (Booth et al. 2002). Booth et al. (2002) have suggested that the extended bloom of *C. socialis* may be the key to the high annual level of primary productivity of the NOW. Furthermore, the bloom of *C. socialis*, much like *Thalassiosira* during the early bloom, may support gonad maturation and spawning of appendicularians up to the end of the productive season of the NOW in September, as well as the relatively high population growth rate of appendicularians in July and September.

In the absence of maturity stage information, a less accurate estimate of spawning time of *F. borealis* can be made. However, its population increase lags that of *O. vanhoeffeni* by ca. 2 months. *Fritillaria borealis* was not detected at any of the stations sampled in April and May. There are moderate abundances in the central NOW in June, at the same stations at which *O. vanhoeffeni* are already at moderate or high abundance, and with a mixture of T-bloom and C-bloom diatom species (Booth et al. 2002). There is ample evidence that *F. borealis* prefers colder, fresher water than do oikopleurid species (Wyatt 1973; Acuña and Anadón 1992; Choe and Deibel 2008). Thus, in the NOW, *F. borealis* population growth follows that for *O. vanhoeffeni*, perhaps due to the inverted seasonal cycle of upper mixed layer salinity in comparison with temperate waters. This temporal pattern is similar to the inverted successional sequence in Conception Bay, Newfoundland, in which *O. vanhoeffeni* peaks in June at the time of the annual salinity maximum, and *F. borealis* in August, during the time of annual declining salinities (Choe and Deibel 2008).

The highest abundances of both *O. vanhoeffeni* and *F. borealis* occur during July and September, in the central and northern NOW, coinciding with the annual, maximum faecal pellet flux in September, when the vertical flux of appendicularian faeces was ca. 35% of the total POC flux (Sampei et al. 2002). At this time, these stations are dominated by BBW, due to the characteristic, fall decrease in southward flow of SRAW through Smith Sound (J.-E. Tremblay, pers. comm.). Available food is dominated by *C. socialis* <10 μm in size (when not in colonial form) in the central and northern NOW and by a mixture of diatoms, flagellates, and dinoflagellates at eastern-central stations (Booth et al. 2002). Companion studies indicate that diatoms are important food for both appendicularians and copepods in July and September (Acuña et al. 2002; Saunders et al. 2003; Stevens et al. 2004).

Abundance and biomass vis-à-vis diatoms and the microbial loop

The rapid reproductive response of *O. vanhoeffeni* to the seasonal proliferation of diatoms contradicts the long-standing paradigm of dependence of appendicularians on small cells of the microbial food web. This older paradigm is being replaced by recent studies of oikopleurid species that indicate dependence of gonad maturation and population growth on diatoms. For example, simulation models suggest that *Oikopleura dioica* needs to encounter relatively high concentrations of diatoms to complete the final stages of gonad maturation (Troedsson et al. 2002; Lombard et al. 2009). Our observations in the NOW suggest a similar dependence of *O. vanhoeffeni* on diatoms for gonad maturation. There is abundant evidence that oikopleurids become mature at different body sizes throughout the year (Wyatt 1973; Choe and Deibel 2009). So, although appendicularians are generally not thought to be food limited (López-Urrutia et al. 2003; Lobón et al. 2013), population growth may be food limited at times due to postponement of the final stages of gonad maturation. Although there was evidence for an important role of diatoms in the maturation and population growth of *O. vanhoeffeni*, late-season production of oikopleurids in the eastern-central NOW (e.g. at stations 40 and 54) and direct observations of diet (Acuña et al. 2002) also demonstrate the supporting role of microbial food webs in sustaining and possibly extending the productive season of appendicularians.

Is *Oikopleura vanhoeffeni* multivoltine in the NOW?

Abundance, trunk length, and maturity stage data provide evidence of two generations of *O. vanhoeffeni* at two stations on the eastern-central side of the NOW (i.e. stations 40 and 54). At station 40, spawning starts in late May or early June, and abundance data suggest that recruitment continues through early September, when the population peaks at ca. 2.5×10^4 ind. m^{-2}. Recruitment appears to be occurring a month or so earlier at stations 54 and 44 (station 44 is on the west side of the NOW, near the mouth of Jones Sound). However, there are two, separate abundance peaks at station 54, one in June and a second in September. Both the abundance and surface-tow trunk length data for station 54 in June (100% <1 mm; *not shown*) support a conclusion of May spawning. Similarly, station 54 abundance data from September samples support a case for additional, late-season spawning in August or early September, when there are no population data samples. It is possible that recruitment at station 40 also occurs in two periods, starting ca. a month later and reaching a peak a couple of weeks earlier than station 54. The above examples support the conclusion that, for this eastern-central region of the NOW, conditions support more than one generation of *O. vanhoeffeni*. However, this conclusion is made cautiously due to the use of population demographic data from summer 1998 and autumn 1999. There is a need to collect appendicularians from a full, single growing season in the future to test this multivoltine hypothesis.

Early spawning of *O. vanhoeffeni* at eastern-central stations is probably encouraged by the relatively early warming and high diatom productivity in the outflow from Inglefield Bay. However, by late June and July, large *O. vanhoeffeni* at these stations were consuming a mixed diet, dominated by diatoms and ciliates, while at more northern and western stations (i.e. stations 1, 2, and 35), prey were almost entirely diatoms (Acuña et al. 2002). Copepod faecal pellet data reported by Saunders et al. (2003) reveal additional evidence for diversification of diets in July and September in the eastern-central NOW, supported by development of a more diverse, microbial loop food web. In addition, fatty acid biomarkers indicate diverse copepod diets in the NOW in September (Stevens et al. 2004).

Is there environmental niche separation between *Oikopleura vanhoeffeni* and *Fritillaria borealis*?

Fritillaria borealis is temporally or spatially separated from oikopleurids, due to differences in preferred environments, generally distinguished by temperature (lower), salinity (lower), the concentration of chlorophyll *a* (lower), or the size of available food particles (smaller) (Wyatt 1973; Acuña and Anadón 1992; Choe and Deibel 2008). However, in the NOW, there is a strong, positive association between *F. borealis* and *O. vanhoeffeni*, with highest abundances of both species at C-bloom stations sampled in July and September. There is no evidence of differential

association of the two species with the major water masses in the NOW. It could not be determined whether there is, or is not, vertical separation between *F. borealis* and *O. vanhoeffeni* in the NOW, as our net tows integrated over broad ranges of depth. In Conception Bay, Newfoundland, there is no vertical separation between the two genera at a scale of 10 s of metres (Choe and Deibel 2008).

In summary, population growth of *O. vanhoeffeni* begins in synchrony with the early diatom bloom (April–May) in BBW, near the Inglefield Bay and Jones Sound polynyas. *F. borealis* begins population growth in June, during transition from the early diatom bloom to the extended bloom of *C. socialis*. Maximum abundance and biomass of both species occur in July and September, at C-bloom stations in BBW. Population doubling time of *O. vanhoeffeni* from April to September is ca. 1 month, a remarkably high rate given the extreme northern latitude. There may be more than one generation of *O. vanhoeffeni* at eastern-central stations, supported by prey from the microbial loop. Although moderate-to-high concentrations of diatoms seem necessary for the initiation of spawning in *O. vanhoeffeni*, there is no statistically significant relationship between abundance and biomass and the concentration of chlorophyll *a*, perhaps due to the coarse-scale, vertical integration of the net tows, as well as to the extended time scale of the study, spanning pre-bloom, bloom, and post-bloom conditions. Spawning and population growth of both species are strongly seasonal, over much of the open water of the NOW (i.e. with a weak spatial pattern). Temperature integrated over the upper 100 m has the strongest effect strength on the abundance and biomass of both species. The association among early-opening polynyas, early and extended diatom production, and high rates of population growth of appendicularians in the NOW, suggests that a warming Arctic will lead to a greater role of these planktonic tunicates in the mortality of polar phytoplankton and microbes, and in the vertical flux of high-quality organic material to deeper water (Bauerfeind et al. 1997; Pesant et al. 1998, 2000).

References

Acuña JL, Anadón R (1992) Appendicularian assemblages in a shelf area and their relationship with temperature. J Plankton Res 9:1233–1250

Acuña JL, Bedo AW, Harris RP, Anadón R (1995) The seasonal succession of appendicularians (Tunicata: Appendicularia) off Plymouth. J Mar Biol Assoc UK 75:755–758. doi:10.1017/s0025315400039187

Acuña JL, Deibel D, Morris CC (1996) Particle capture mechanism of the pelagic tunicate *Oikopleura vanhoeffeni*. Limnol Oceanogr 41:1800–1814

Acuña JL, Deibel D, Bochdansky AB, Hatfield E (1999) *In situ* ingestion rates of appendicularian tunicates in the Northeast Water Polynya (NE Greenland). Mar Ecol Prog Ser 186:149–160

Acuña JL, Deibel D, Saunders PA, Booth B, Hatfield E, Klein B, Mei Z-P, Rivkin RB (2002) Phytoplankton ingestion by appendicularians in the North Water. Deep Sea Res II 49:5101–5115

Aksenov Y, Bacon S, Coward AC, Holliday NP (2010) Polar outflow from the Arctic Ocean: a high resolution model study. J Mar Syst 83:14–37. doi:10.1016/j.jmarsys.2010.06.007

Arashkevich E, Wassmann P, Pasternak A, Riser CW (2002) Seasonal and spatial changes in biomass, structure, and development progress of the zooplankton community in the Barents Sea. J Mar Syst 38:125–145

Ardynya M, Gosselin M, Michel C, Poulin M, Tremblay J-É (2011) Environmental forcing of phytoplankton community structure and function in the Canadian high arctic: contrasting oligotrophic and eutrophic regions. Mar Ecol Prog Ser 442:37–57. doi:10.3354/meps09378

Bâcle J, Carmack EC, Ingram RG (2002) Water column structure and circulation under the North Water during spring transition: April–July 1998. Deep Sea Res II 49:4907–4925

Bauerfeind E, Garrity C, Krumbholz M, Ramseier RO, Voß M (1997) Seasonal variability of sediment trap collections in the Northeast Water Polynya. Part 2. Biochemical and microscopic composition of sedimenting matter. J Mar Syst 10:371–389

Berreville OF, Vézina AF, Thompson KR, Klein B (2008) Exploratory data analysis of the interactions among physics, food web structure, and function in two Arctic polynyas. Can J Fish Aquat Sci 65:1036–1046. doi:10.1111/j.1748-7692.2007.00101.x

Blachowiak-Samolyk K, Søreide JE, Kwasniewski S, Sundfjord A, Hop H, Falk-Petersen S, Hegseth EN (2008) Hydrodynamic control of mesozooplankton abundance and biomass in northern Svalbard waters (79–81°N). Deep Sea Res II 55:2210–2224. doi:10.1016/j.dsr2.2008.05.018

Booth BC, Larouche P, Bélanger S, Klein B, Amiel D, Mei Z-P (2002) Dynamics of *Chaetoceros socialis* blooms in the North Water. Deep Sea Res II 49:5003–5025

Capitanio FL, Curelovich J, Tresguerres M, Negri RM, Viñas MD, Esnal GB (2008) Seasonal cycle of appendicularians at a coastal station (38°28′S, 57°41′W) of the SW Atlantic Ocean. Bull Mar Sci 82:171–184

Choe N, Deibel D (2008) Temporal and vertical distributions of three appendicularian species (Tunicata) in Conception Bay, Newfoundland. J Plankton Res 30:969–979. doi:10.1093/plankt/fbn064

Choe N, Deibel D (2009) Statolith diameter as an age indicator in the planktonic tunicate *Oikopleura vanhoeffeni*: variability in age-specific growth patterns in Conception Bay, Newfoundland. J Exp Mar Biol Ecol 375:89–98. doi:10.1016/j.jembe.2009.05.013

Choe N, Deibel D (2011) Life history characters and population dynamics of the boreal larvacean *Oikopleura vanhoeffeni*

(Tunicata) in Conception Bay, Newfoundland. J Mar Biol Assoc UK 91:1587–1598. doi:10.1017/S0025315410001876

Deibel D (1988) Filter feeding by *Oikopleura vanhoeffeni*: grazing impact on suspended particles in cold ocean waters. Mar Biol 99:177–186

Deibel D (1998) Feeding and metabolism of Appendicularia. In: Bone Q (ed) Biology of pelagic tunicates. Oxford University Press, Oxford, pp 139–150

Deibel D, Saunders PA, Acuña JL, Bochdansky AB, Shiga N, Rivkin RB (2005) The role of appendicularian tunicates in the biogenic carbon cycle of three Arctic polynyas. In: Gorsky G, Youngbluth YG, Deibel D (eds) Response of marine ecosystems to global change: ecological impact of appendicularians. Éditions Scientifiques, Paris, pp 327–358

Deming JW, Fortier L, Fukuchi M (2002) The international North Water Polynya Study (NOW): a brief overview. Deep Sea Res II 49:4887–4892

Dvorestsky VG, Dvorestsky AG (2013) Structure of mesozooplankton community in the Barents Sea and adjacent waters in August 2009. J Nat Hist 47:2095–2114. doi:10.1080/00222933.2013.772670

Dvoretsky VG, Dvoretsky AG (2009) Summer mesozooplankton structure in the Pechora Sea (south-eastern Barents Sea). Estuar Coast Shelf Sci 84:11–20. doi:10.1016/j.ecss.2009.05.020

Fenaux R (1961) Existence d'un ordre cyclique d'abondance relative maximale chez les appendiculaires de surface (tuniciers pélagiques). C R Hebd Séances Acad Sci 253:2271–2273

Fenaux R (1976) Cycle vital, croissance et production chez *Fritillaria pellucida* (Appendicularia), dans la baie de Villefranche-sur-Mer, France. Mar Biol 34:229–238

Fenaux R, Bone Q, Deibel D (1998) Appendicularia distribution and zoogeography. In: Bone Q (ed) The biology of pelagic tunicates. Oxford University Press, Oxford, pp 251–264

Fernández D, López-Urrutia Á, Fernández A, Acuña JL, Harris R (2004) Retention efficiency of 0.2–6 μm particles by the appendicularians *Oikopleura dioica* and *Fritillaria borealis*. Mar Ecol Prog Ser 266:89–101

Flood PR (2003) House formation and feeding behaviour of *Fritillaria borealis* (Appendicularia: Tunicata). Mar Biol 143:467–475. doi:10.1007/s00227-003-1075-y

Flood PR, Deibel D, Morris CC (1992) Filtration of colloidal melanin from sea water by planktonic tunicates. Nature 355:630–632

Hopcroft RR, Roff JC (1995) Zooplankton growth rates; extraordinary production by the larvacean *Oikopleura dioica* in tropical waters. J Plankton Res 17:205–220

Hopcroft RR, Kosobokova K, Pinchuk AI (2010) Zooplankton community patterns in the Chukchi Sea during summer 2004. Deep Sea Res II 57:27–39. doi:10.1016/j.dsr2.2009.08.003

Howell SEL, Tivy A, Agnew T, Markus T, Derksen C (2010) Extreme low sea ice years in the Canadian arctic archipelago: 1998 versus 2007. J Geophys Res 115:C10053. doi:10.1029/2010JC006155

Ingram RG, Bâcle J, Barber DG, Gratton Y, Melling H (2002) An overview of physical processes in the North Water. Deep Sea Res II 49:4893–4906

Klein B, LeBlanc B, Mei Z-P et al (2002) Phytoplankton biomass, production and potential export in the North Water. Deep Sea Res II 49:4983–5002

Knoechel R, Steel-Flynn D (1989) Clearance rates of *Oikopleura* in cold coastal Newfoundland waters: a predictive model and its trophodynamic implications. Mar Ecol Prog Ser 53:257–266

Lobón CM, Bouquet JM, Reeve M, Novac A, Acuña JL, Thompson EM (2013) Response of the pelagic tunicate appendicularian, *Oikopleura dioica* to controlled simulations of a strong bloom condition: a bottom-up perspective. Limnol Oceanogr 58:215–226. doi:10.4319/lo.2013.58.1.0215

Lombard F, Sciandra A, Gorsky G (2009) Appendicularian ecophysiology. II. Modeling nutrition, metabolism, growth and reproduction of the appendicularian *Oikopleura dioica*. J Mar Syst 78:617–629. doi:10.1016/j.jmarsys.2009.01.004

López-Urrutia A, Acuña JL, Irigoien X, Harris RP (2003) Food limitation and growth in temperate epipelagic appendicularians (Tunicata). Mar Ecol Prog Ser 252:143–157. doi:10.3354/meps252143

Lovejoy C, Legendre L, Martineau M-J, Bâcle J, von Quillfeldt CH (2002) Distribution of phytoplankton and other protists in the North Water. Deep Sea Res II 49:5027–5047

Marsden RF, Serdula J, Key E, Minnett PJ (2004) Are polynyas self-sustaining? Atmos Ocean 42:251–265

Mei Z-P, Legendre L, Gratton Y et al (2002) Physical control of spring-summer phytoplankton dynamics in the North Water, April–July 1998. Deep Sea Res II 49:4959–4982

Melling H, Gratton Y, Ingram G (2001) Ocean circulation within the North Water Polynya of Baffin Bay. Atmos Ocean 39:301–325

Nakamura Y (1998) Blooms of tunicates *Oikopleura* spp. and *Dolioletta gegenbauri* in the Seto Inland Sea, Japan, during summer. Hydrobiol 385:183–192

Odate T, Hirawake T, Kudoh S, Klein B, LeBlanc B, Fukuchi M (2002) Temporal and spatial patterns in the surface-water biomass of phytoplankton in the North Water. Deep Sea Res II 49:4947–4958

Pesant S, Legendre L, Gosselin M et al (1998) Pathways of carbon cycling in the euphotic zone: the fate of large-sized phytoplankton in the Northeast Water Polynya. J Plankton Res 20:1267–1291

Pesant S, Legendre L, Gosselin M, Bjornsen PK, Fortier L, Michaud J, Nielsen TG (2000) Pathways of carbon cycling in marine surface waters: the fate of small-sized phytoplankton in the Northeast Water Polynya. J Plankton Res 22:799–801. doi:10.1093/plankt/22.4.779

Post E, Bhatt US, Bitz CM, Brodie JF, Fulton TL, Hebblewhite M, Kerby J, Kutz SJ, Stirling I, Walker DA (2013) Ecological consequences of sea-ice decline. Science 341:519–524. doi:10.1126/science.1235225

Rabe B, Johnson HL, Münchow A, Melling H (2012) Geostrophic ocean currents and freshwater fluxes across the Canadian polar shelf via Nares Strait. J Mar Res 70:603–640

Rasmussen TAS, Kleim N, Kaas E (2011) The effect of climate change on the sea ice and hydrography of Nares Strait. Atmos Ocean 49:245–258. doi:10.1080/07055900.2011.604404

Richard PR, Heide-Jørgensen MP, St. Aubin D (1998a) Fall movements of belugas (*Delphinapterus leucas*) with satellite-linked transmitters in Lancaster Sound, Jones Sound, and northern Baffin Bay. Arctic 51:5–16

Richard PR, Orr JR, Dietz R, Dueck L (1998b) Sightings of belugas and other marine mammals in the North Water, Late March 1993. Arctic 51:1–4

Ringuette M, Fortier L, Fortier M, Runge JA, Bélanger S, Larouche P, Weslawski J-M, Kwasniewski S (2002) Advanced recruitment and accelerated population development in Arctic calanoid copepods of the North Water. Deep Sea Res II 49:5081–5099

Sampei M, Sasaki H, Hattori H, Kudoh S, Kashino Y, Fukuchi M (2002) Seasonal and spatial variability in the flux of biogenic particles in the North Water, 1997–1998. Deep Sea Res II 49:5245–5257

Saunders PA, Deibel D, Stevens CJ, Rivkin RB, Lee SH, Klein B (2003) Copepod herbivory rate in a large arctic polynya and its relationship to seasonal and spatial variation in copepod and phytoplankton biomass. Mar Ecol Prog Ser 261:183–199

Shiga N (1976) Maturity stages and relative growth of *Oikopleura labradoriensis* Lohmann (Tunicata, Appendicularia). Bull Plankton Soc Jpn 23:81–95

Shiga N (1993) Regional and vertical distributions of *Oikopleura vanhoeffeni* on the northern Bering Sea shelf in summer. Bull Plankton Soc Jpn 39:117–126

Shiga N, Shogo T, Nishiuchi K (1998) Interannual variation and vertical distribution of appendicularians in the south of St. Lawrence Island, northern Bering Sea shelf, in summer. Mem Fac Fish Hokkaido Univ 45:48–51

Skjoldal HR, Johannesen P, Klinken J, Halvorsen H (1993) Controlled ecosystem experiment in Lindåspollene, western Norway, June 1979: comparisons between natural and two enclosed water columns. Sarsia 68:47–64

Stevens CJ, Deibel D, Parrish CC (2004) Copepod omnivory in the North Water Polynya (Baffin Bay) during autumn: spatial patterns in lipid composition. Deep Sea Res I 51:1637–1658. doi:10.1016/j.dsr.2004.07.011

Stewart REA (2008) Redefining walrus stocks in Canada. Arctic 61:292–308

Stirling I (1997) The importance of polynyas, ice edges, and leads to marine mammals and birds. J Mar Syst 10:9–21

Tamura T, Oshima KI (2011) Mapping of sea ice production in the Arctic coastal polynyas. J Geophys Res 116:C07030. doi:10.1029/2010JC006586

Tang CCL, Ross CK, Yao T, Petrie B, DeTracey BM, Dunlap E (2004) The circulation, water masses and sea-ice of Baffin Bay. Prog Oceanogr 63:183–228. doi:10.1016/j.pocean.2004.09.005

Thiemann GW, Iverson SJ, Stirling I (2007) Variability in the blubber fatty acid composition of ringed seals (*Phoca hispida*) across the Canadian Arctic. Mar Mammal Sci. 23:241–261. doi:10.1111/j.1748-7692.2007.00101.x

Tönnesson K, Maar M, Vargas C et al (2005) Grazing impact of *Oikopleura dioica* and copepods on an autumn plankton community. Mar Biol Res 1:365–373

Tremblay J-É, Gratton Y, Carmack EC, Payne CD, Price NM (2002a) Impact of the large-scale Arctic circulation and the North Water Polynya on nutrient inventories in Baffin Bay. J Geophys Res. doi:10.1029/2000JC000595

Tremblay J-É, Gratton Y, Fauchot J, Price NM (2002b) Climatic and oceanic forcing of new, net, and diatom production in the North Water. Deep Sea Res II 49:4927–4946

Tremblay J-É, Michel C, Hobson KA, Gosselin M, Price NM (2006) Bloom dynamics in early opening waters of the Arctic Ocean. Limnol Oceanogr 51:900–912

Troedsson C, Bouquet JM, Aksnes DL, Thompson EM (2002) Resource allocation between somatic growth and reproductive output in the pelagic chordate *Oikopleura dioica* allows opportunistic response to nutritional variation. Mar Ecol Prog Ser 243:83–91. doi:10.3354/meps243083

Vidussi F, Roy S, Lovejoy C, Gammelgaard M, Thomsen HA, Booth B, Tremblay J-É, Mostajir B (2004) Spatial and temporal variability of the phytoplankton community structure in the North Water Polynya, investigated using pigment biomarkers. Can J Fish Aquat Sci 61:2038–2052. doi:10.1139/F04-152

Wilson KJ, Barber DG, King DJ (2001) Validation and production of RADARSAT-1 derived ice-motion maps in the North Water (NOW) polynya, January–December 1998. Atmos Ocean 39:257–278. doi:10.1080/07055900.2001.9649680

Wyatt T (1973) The biology of *Oikopleura dioica* and *Fritillaria borealis* in the Southern Bight. Mar Biol 22:137–158